Spring 5-31-2017

III-nitride nanowire light-emitting diodes: design and characterization

Dipayan Datta Choudhary
New Jersey Institute of Technology

Copyright Warning & Restrictions

The copyright law of the United States (Title 17, United States Code) governs the making of photocopies or other reproductions of copyrighted material.

Under certain conditions specified in the law, libraries and archives are authorized to furnish a photocopy or other reproduction. One of these specified conditions is that the photocopy or reproduction is not to be "used for any purpose other than private study, scholarship, or research." If a, user makes a request for, or later uses, a photocopy or reproduction for purposes in excess of "fair use" that user may be liable for copyright infringement,

This institution reserves the right to refuse to accept a copying order if, in its judgment, fulfillment of the order would involve violation of copyright law.

Please Note: The author retains the copyright while the New Jersey Institute of Technology reserves the right to distribute this thesis or dissertation

Printing note: If you do not wish to print this page, then select "Pages from: first page # to: last page #" on the print dialog screen

ABSTRACT

III-NITRIDE NANOWIRE LIGHT-EMITTING DIODES: DESIGN AND CHARACTERIZATION

by
Dipayan Datta Choudhary

III-nitride semiconductors have been intensively studied for optoelectronic devices, due to the superb advantages offered by this materials system. The direct energy bandgap III-nitride semiconductors can absorb or emit light efficiently over a broad spectrum, ranging from 0.65 eV (InN) to 6.4 eV (AlN), which encompasses from deep ultraviolet to near infrared spectrum. However, due to the lack of native substrates, conventional III-nitride planar heterostructures generally exhibit very high dislocation densities that severely limit the device performance and reliability. On the other hand, nanowire heterostructures can be grown on lattice mismatched substrates with drastically reduced dislocation densities, due to highly effective lateral stress relaxation. Nanowire light-emitting diodes (LEDs) with emission in the ultraviolet to visible wavelength range have recently been studied for applications in solid-state lighting, flat-panel displays, and solar-blind detectors. In this thesis, investigation of the systematic process flow of design and epitaxial growth of group III-nitride nanoscale heterostructures was done. Moreover, demonstration of phosphor-free nanowire white LEDs using InGaN/AlGaN nanowire heterostructures grown directly on Si(111) substrates by molecular beam epitaxy was made. Full-color emission across nearly the entire visible wavelength range was realized by controlling the In composition in the InGaN active region. Strong white-light emission was recorded for the unpackaged nanowire LEDs with an unprecedentedly high color rendering index of 98. Moreover, LEDs with the operating wavelengths in the ultraviolet (UV) spectra, with emission wavelength in the range of 280-320 nm (UV-B) or shorter wavelength hold tremendous promise for applications in phototherapy, skin treatments, high

speed dissociation and high density optical recording. Current planar AlGaN based UV-B LEDs have relatively low quantum efficiency due to their high dislocation density resulted from the large lattice mismatch between the AlGaN and suitable substrates. In this study, associated with the achievement of visible LEDs, the development of high brightness AlGaN/GaN nanowire UV-LEDs via careful design and device fabrication was shown. Strong photoluminescence spectra were recorded from these UV-B LEDs. The emission peak can be tunable from 290 nm to 320 nm by varying the Al content in AlGaN active region which can be done by optimizing the growth condition including Al/Ga flux ratio and also the growth temperature. Such visible to UV-B nanowire LEDs are ideally suited for future smart lighting, full-color display, phototherapy and skin treatments applications.

III-NITRIDE NANOWIRE LIGHT-EMITTING DIODES: DESIGN AND CHARACTERIZATION

by
Dipayan Datta Choudhary

A Thesis
Submitted to the Faculty of
New Jersey Institute of Technology and
in Partial Fulfillment of the Requirements for the Degree of
Masters of Science in Energy and Power Systems

Helen and John C. Hartmann Department of
Electrical and Computer Engineering

May 2017

APPROVAL PAGE

III-NITRIDE NANOWIRE LIGHT-EMITTING DIODES: DESIGN AND CHARACTERIZATION

Dipayan Datta Choudhary

Dr. Hieu Pham Trung Nguyen, Thesis Advisor — Date
Assistant Professor of Electrical and Computer Engineering, NJIT

Dr. Marek Sosnowski, Committee Member — Date
Associate Chair of Undergraduate Study of Electrical and Computer Engineering,
Professor of Electrical and Computer Engineering, NJIT

Dr. Leonid Tsybeskov, Committee Member — Date
Chair of Electrical and Computer Engineering, Professor of Electrical and
Computer Engineering, NJIT

BIOGRAPHICAL SKETCH

Author: Dipayan Datta Choudhary

Degree: Masters of Science

Date: May 2017

Undergraduate and Graduate Education:

- Masters in Power Systems and Energy,
  New Jersey Institute of Technology, Newark, NJ, 2017
- B.Tech,
  National Institute of Technology Warangal India, 2009

Major: Energy and Power Systems

Presentations and Publications:

Peer Reviewed Papers

D.D. Choudhary, M. R. Philip, M.N. Bhuyian, M. Djavid, and H.P.T. Nguyen, "Optical and Electrical Characteristics of AlGaN Nanowire Light-Emitting Diodes Operating in the Ultraviolet B Wavelength" , In preparation

M. R. Philip, D.D. Choudhary, M. Djavid, and H.P.T. Nguyen, "III-Nitride nanowire Light-Emitting Diodes on Metal Substrates: Direct-Substrate-Transferring Approach for Flexible Photonics," *Nanoscale (The Royal Society of Chemistry)*, Under Review

M. Djavid, M. H. T. Dastjerdi, M. R. Philip, D. D. Choudhary And H. P. T. Nguyen, "Photonic Crystal Based Permutation Switch for Optical Networks," *Journal of Electronic Materials (JEMS)*, Under review

M. Djavid , D. D. Choudhary, M. R. Philip, and H. P. T. Nguyen , "Effects of the optical absorption in deep ultraviolet nanowire light emitting diodes," *Photonics and Nanostructures: Fundamentals and Applications*, Under review

M. Djavid, M. H. T. Dastjerdi, M. R. Philip, D. D. Choudhary, A. Khreishah, and H. P. T. Nguyen, "4-Port Reciprocal Optical Circulators Employing Photonic Crystals for Integrated Photonics Circuits," *Optik International Journal for Light and Electron Optics* , Under review

M. R. Philip, D.D. Choudhary, M. Djavid, M.N. Bhuyian and H.P.T. Nguyen, "Controlling Color Emission of InGaN/AlGaN Nanowire Light Emitting Diodes Grown by Molecular Beam Epitaxy," *Journal of Vacuum Science and Technology - B* , 35 (2017), 02B108 Featured as Editor's pick in JVST B in March 2017

Conferences

M. R. Philip, D. D. Choudhary, M. Djavid, M. N. Bhuyian, D. Misra, J. Piao, and H. P. T. Nguyen, "Phosphor-Free III-Nitride Nanowire Light-Emitting Diodes on Flexible Substrates, *The 11th International Symposium on Semiconductor Light Emitting Diodes, Banff, Canada*, October 8-10, 2017

M. R. Philip, D. D. Choudhary, M. Djavid, M. N. Bhuyian, J. Piao, and H. P. T. Nguyen, "Controlling Color Emission of InGaN/AlGaN Nanowire Light Emitting Diodes Grown by Molecular Beam Epitaxy," *32nd North American Molecular Beam Epitaxy Conference Saratoga Springs, New York* , September 18-21, 2016

I dedicate this effort to my mother, father and brother, who have always supported me throughout my life.

'Live long and prosper'

Spock

ACKNOWLEDGMENT

This effort would not be possible without the help of my professor Dr. Hieu Pham Trung Nguyen. He has shaped my career and shown me the light of academia. I have never enjoyed education as much as I have under him. His passion for research and visionary speeches have molded me into a visionary myself, I am truly a student of science now!

I would like to thank Dr. Marek Sosnowski and Dr. Leonid Tsybeskov for their kind assistance in our experiments, and agreeing to spend their valuable time to be my committee members.

I would like to thank the members in my research group, Dr. Mehrdad Djavid and Mr. Moab Rajan Philip and Dr. Md Nasiruddin Bhuyian. They were my support system, teachers, friends and really helped my transition into the field of research from engineering.

The department of Electrical and Computer Engineering at New Jersey Institute of Technology and its administration run by, Tanita, Barbara, Ellen and Joan, who help run it so smoothly were of great help, and without them, students like me would never be able to do just our research, they keep so much off our plates.

The Global Students Office has been of immense help, especially to a foreign student such as myself. They always were available to remind of what I had to do to maintain the status of a student, and provide great assistance to all foreign students.

I would like to take this opportunity to thank my friends, Sunit, Pritish, Harsha, Aakash, Fiona, Ram, Akshay, Ajibola, and Suyog with whom I spend so much time with during my masters program. A special shoutout to my soccer team, Abid, Unni, Biru, Raul and Abilash! Without you guys, there is no fun in putting so much effort, because after 5 days of tirelessly waiting for experiments to show signs of life, one needs a pat in the back.

Last but not least, I would like to thank Dr. Mengchu Zhou, my academic adviser, for telling me about this opportunity and how to achieve it. Sir, you truly have helped in making this masters program a worthwhile one, thank you.

TABLE OF CONTENTS

TABLE OF CONTENTS
(Continued)

Chapter **Page**

LIST OF TABLES

Table **Page**

LIST OF FIGURES

LIST OF FIGURES
(Continued)

Figure **Page**

CHAPTER 1

INTRODUCTION

High performance light-emitting diode (LED) devices with high efficiency and stability are highly expected for numerous applications ranging from general lighting, displays to applications in photo-therapy [27], skin treatments[26], high speed dissociation [17]and high density optical recording[12]. The LEDs have become important parts of our everyday activities and are widely used around us. Lighting technology has been slowly shifting to LEDs, for instance, displays on our TVs, mobile devices, and general indoor/outdoor lighting. LEDs have been useful in many other domains as well, such as:

Ultraviolet LEDs (UV LEDs): 240 to 360 nm Uses of UV LEDs are wide and varied. They range from industrial curing applications, water disinfection and medical/bio-medical uses. The primary material used for the fabrication of UV LEDs is gallium nitride/aluminum gallium nitride (GaN/AlGaN).

Below are some of the other specific applications of UV LEDs:

- Medical use (sterilization, skin care, discrimination of cancer) - deep UV LEDs (300 - 350 nm)
- High speed dissociation of pollutant materials (UV LED array 260 - 340 nm)
- Semiconductor illumination (260 - 340 nm)
- LASER for high-density optical recording (250 -300 nm)
- For generating vitamin D in our body through the exposure to the UV-B (290 320 nm) range of wavelength.

Near UV to green LEDs: (395 to 530 nm) The material generally used for the fabrication of LEDs in this range is Indium Gallium Nitride (InGaN) at varied compositions. Blue LEDs of (450 to 475 nm) are widely manufactured for making phosphorous based white light, and on green LEDs (520 to 530 nm) for traffic signals.

Yellow green to red LEDs: (565 to 645 nm) Aluminum Indium Gallium Phosphide (AlInGaP) is generally used to manufacture LEDs of this wavelength. Yellow LEDs (590 nm) and red LEDs (625 nm) are used for traffic signals widely.

Deep red to near infrared: (660 to 900 nm) LEDs at this range are usually manufactured using Aluminum Gallium Arsenide (AlGaAs) or Gallium Arsenide (GaAs) and their variations. These LEDs are used for communication purposes such as infrared remote controls, night-vision illumination, industrial photo controls and various medical applications.

With such a wide array of uses and high practical impact, it is an absolute scientific necessity to keep improving the attributes of LEDs from a fundamental point of view. The basic questions leading into our research were question which challenged how a LED functions at an atomic level, hence we have taken a quantum approach in improving the fundamental attributes of LEDs. Hence, we have grown nanowire LEDs. This thesis reports the development of nearly defect free nanowire UV LEDs operating in the UV-B region (280-315 nm) to visible color composed of group III-nitride nanoscale heterostructures.

Group III-nitride nanowire heterostructures, in recent years have been extensively studied due to their numerous advantages. These compound semiconductors show unique optical and electrical behavior, such as, good thermal conductivity, high electron mobility, high breakdown electric field, large saturation velocity and extreme chemical stability. [21] This material has a tunable band gap ranging from 0.65 eV (InN) to 6.4 eV (AlN), which almost comprises of the entire solar spectrum.

The growth and progress of the III-nitride based conventional planar structures have been hindered due to the following reasons:

- Lack of high quality and low cost GaN substrates
- Necessitating epitaxy on substrates with large lattice mismatch
- Green gap referring to the poor efficiency of green, yellow and red LEDs, preventing the achievement of high performance phosphor-free white LEDs
- Efficiency droop droop in efficiency at high injection currents

The last two reasons can be attributed to the high-density dislocations caused by lattice-mismatched epitaxy.

1.1 Advantages of LEDs over other Lighting Technologies

LED lamps or light sources which are fitted with LEDs as the source of light, have numerous advantages associated with them. LED lamps have a greater life span and higher efficiency compared to other light sources. LED lamps, since they are semiconductors, are very favorable when it comes to continuous on-off cycling. Certain LED lamps have shown exceptionally stable luminous flux output. LED lamps are more robust, making them easier for transportation purposes and handling. Moreover, tailoring various properties of LED lamps to meet the needs of applications is relatively straight forward. These properties include dimensions of the illuminating area, angular distribution of radiation, and the shape of the emission spectrum. Furthermore, the spectra of most white LED lamps unlike those of incandescent lamps do not extend needlessly to the UV or the infrared (IR) regions. [31] However, the disadvantage is that it is expensive as of now.

There are publications showing how vital LED lighting is to the overall energy consumption and how much that in turn would affect the environment. [25]

Table 1.1 Comparing the Indicators of the Different Light Sources Relative to the Incandescent Light Bulb

	Daily 6 hours of operation	*Halogen light bulb*	*Compact fluorescent*	*LED light source*
(i)	Investment needed	2.27	9.09	64.77
(ii)	Discounted payback time in years	0.33	0.42	3.25
(iii)	Lifespan	0.93	4.63	5.56
(iv)	Cost saving compared to incandescent light bulb in USD a tear	4.52	22.02	13.41
(v)	Cost saving compared to incandescent light bulb (percent)	15.2	74.3	45.2
(vi)	Energy saving compared to incandescent light bulb (percent)	30	81.7	80

Table 1.1 shows a comparison of different types of light sources and their financial viability [25]. It is reported that, there is around 80 percentage energy saved using LEDs as a lighting source as opposed to incandescent light bulbs, which we have been using for a long time now. This study demonstrates how the lighting industry is moving forward. With LED lighting taking over most conventional sources of light like incandescent lighting, the scientific progress made in LED lighting has been exponential in recent years. Therefore high power/high efficiency LED lamps are highly desired for our lighting technology. In this regard, one of the most novel ideas is using nanowire semiconductors, which have been proved as promising light source that can outperform the current thin-film counterparts. In the following sections, discussion on why nanowires are becoming a forerunner in modern day lighting will be looked upon.

1.2 Description of Nanowires and Nanowire LEDs

Nanowire is a nanostructure in a wire form, with the diameter in the order of nanometer. It can also be defined as the ratio of the length to width being greater than 1000. At these scales, quantum mechanical effects are important which coined the term "quantum wires" -(Wiki - Nanowire).

A nanowire LED is an array of nanowires, of which each nanowire has a p-doped, n-doped and an active region within itself. III-nitride semiconductor heterostructures, for example, consist of layers of GaN and AlGaN/InGaN stacked on top of each other at particular dimensions and varied compositions to enable a quantum light trapping effect. The emitting wavelength of the nanowire LEDs is mostly defined by the composition of the semiconductor materials in the device active region.

1.3 Why Nanowires?

The last 50 years of research of silicon photo-voltaic (PV) devices have led us to around 20% efficiency. There are PVs of higher efficiency as we shall discuss, but they are not commercial but for particular needs and requirements. The main reason for the non-popularity is the cost. Si wafer requires extensive purification to maintain a reasonable performance. We have come to an understanding in the industry and research and development around the globe, that, Si is reaching a limit. We are in a requirement to continuously make our technology faster and more efficient at a reduced cost. Thus, grew the interest of nanowires along with a plethora of other new ideas. Figure 1.1 shows nanowires grown on silicon substrate.

The dimension of nanowires, which is demonstrated from Figure 1.1, enable electrons and photons to experience quantum confinement effects, which we utilize in our structure. Yet, since one of the dimension (length) can range into microns or even longer, it makes it possible for them to connect with other macroscopic devices and the outside world. The simple structure of the nanowire makes it very easy to

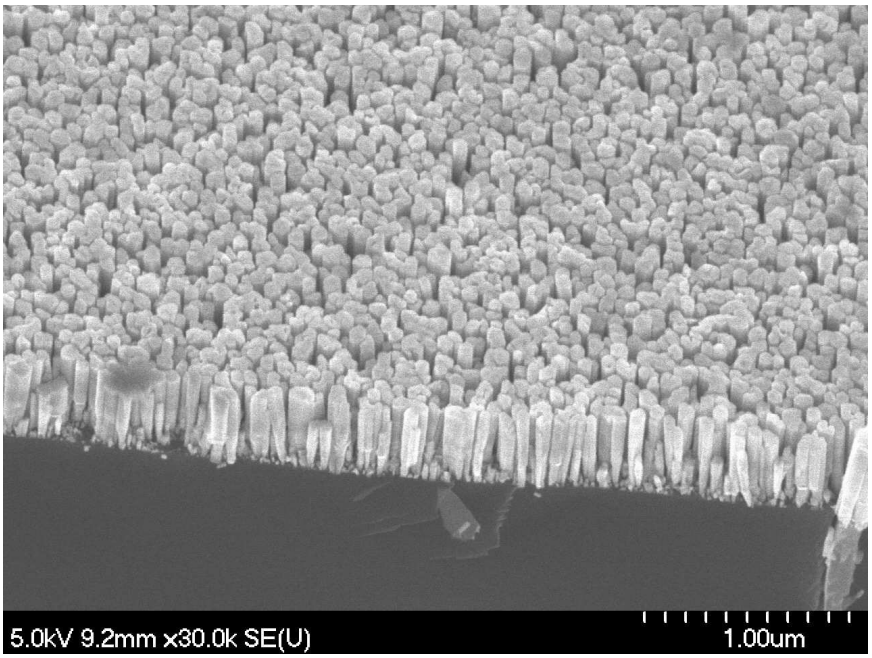

Figure 1.1 SEM image showing nanowires grown on Silicon substrate.

grow them with significantly reduced defect densities, and electrons pass through unhindered. Nearly defect-free nanowire structures promise significant performance advantages in the photovoltaic processes, including light absorption, electron-hole pair generation, and charge carrier separation and collection [32][28][4][5][34]. For example, nanowire arrays can introduce light trapping effect, which can dramatically enhance the light absorption. In addition, nanowire devices can be fabricated on extremely low-cost substrates, including aluminum foil and amorphous glass. This issue can be seen in growing of Si, which always have defects [38]. Additionally, the structure enables the growth of materials together that normally don't mix easily. Nanowire LEDs have proven to show improvement in internal quantum efficiency and light extraction efficiency constantly, leading to be a serious candidate to be a feasible means of producing light in the future.

We have utilized this structure as fundamental platform for producing light emitters including LEDs and laser diodes.

1.3.1 How Nanowire LEDs Work?

A nanowire LED array consisting of multiple nanowire LEDs that can be used to generate light. Each nanowire is capable of producing light of desired wavelength mostly depending on the band gap energy in the device active region. A nanowire LED typically consists of three major parts.

- p-type region,
- Active region, and
- n-type region.

The structure resembles a typical semiconductor heterojunction. A representation of the electron and hole dynamics is shown in Figure 1.2. Figure 1.2 shows a schematic of the LED current components injected into the device's active region. We use an ABF model to study the various carrier recombination processes [19]. The internal quantum efficiency of GaN-based LED is,

$$\eta_i = \frac{BN^2}{AN + BN^2 + f(N)} \tag{1.1}$$

Assuming unity electrical injection efficiency, η_i is the internal quantum efficiency, N is the carrier density and A, and B are the Shockley-Read-Hall nonradiative recombination and radiative recombination coefficients. Auger recombination and any other high order carrier loss processes are described by f(N). f(N) also represents the carrier leakage outside the active region. [19]

Figure 1.2 shows the schematic structure of a single nanowire LED structure. The active region emits light of a frequency depending on the band gap of the material.

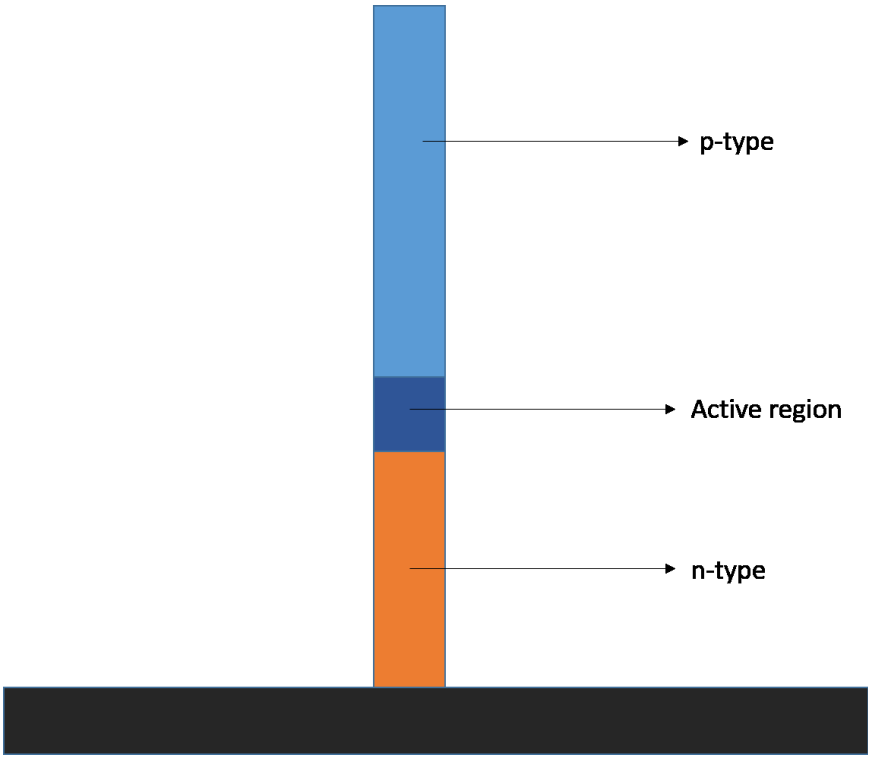

Figure 1.2 Schematic structure of a typical nanowire structure.

1.4 Current Problems with Nanowire LEDs?

Currently, external quantum efficiency (EQE) and light extraction efficiency (LEE) of III-nitirde nanowire LEDs have remained issues and need to be improved. LEE and EQE are priority factors which determine the usability of nanowire LEDs. Further discussion on the relation to device performance and these factors are mentioned in further sections. The solution to these issues lie in the understanding of how the structure and its dimensions are related to problems such as lattice strain, enhanced light trapping, band gap tuning, output power to name a few.

There is a lack of native substrates, conventional III-nitride planar heterostructures generally exhibit very high dislocation densities that severely limit the device performance and reliability. The performance of traditional quantum well based LEDs have been limited due to the presence of large dislocation densities and strain-induced polarization field associated with large inter-layer lattice mismatch.

Nanowires provide a solution to these issues because of the effective lateral stress relaxation [21]. One of the major concerns about using InGaN based LEDs for commercial applications is the efficiency droop. This degradation occurs at high injection currents, and hence is difficult to achieve high brightness and high power lighting when operating at these current levels. Extensive investigation is taking place to tackle this issue. Carrier delocalization [20], polarization field [16], Auger recombination [10], carrier leakage [30] and poor hole transport [6] are some of the reasons identified attributing to this efficiency droop. [21]

The following sections will describe these phenomena which attributes to low efficiency, or in other words, efficiency droop, in nanowire LEDs in detail.

1.4.1 Efficiency Droop

A principal advantage of LED lighting is high energy efficiency compared to conventional lighting technologies. However, when it comes to GaN-based LEDs, at high current injection that is practically required in practical scenarios, the LED efficiency is greatly reduced, especially for LEDs operating in the green or longer wavelength regions. [24]

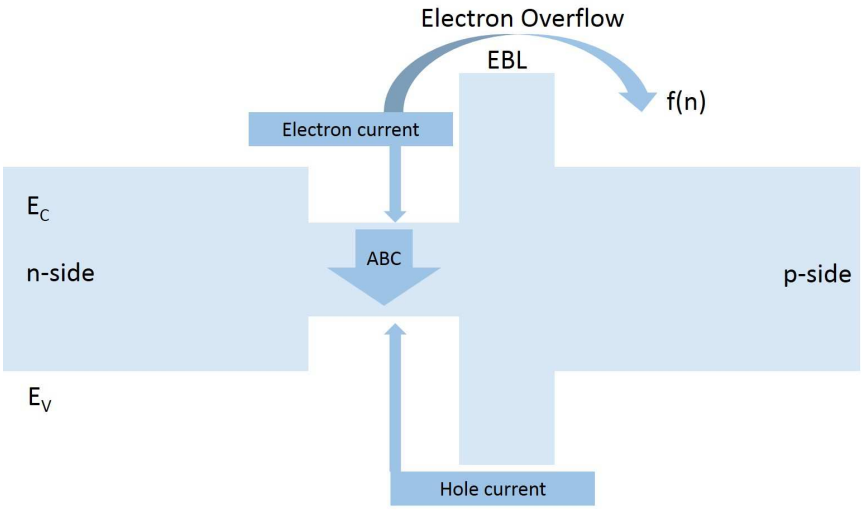

Figure 1.3 Illustration of current injection components in an LED device.

Figure 1.3 shows how the ABF model is related to input current. E_c represents the conduction band, E_v represents the valence band and EBL represents the eletron blocking layer. This, in accordance with equations 1.2 to 1.4 can help us understand why this efficiency droop occurs over a wide range of wavelengths, from UV to green. [19]

LED efficiency is ideally 100% when every single injected electron generated a photon that is emitted from the LED. But, this is a theoretical scenario, excluding the electrical to optical energy conversion accompanies losses during the process.

$$\eta_{EQE} = \eta_{IQE} X \eta_{EXE} X \eta_{inj} \tag{1.2}$$

η_{EXE} is the optical extraction efficiency, and is defined as the ratio of photons emitted from the LED to the photons generated in the LED quantum wells active region, hence, it counts for the photons lost inside the LED.

η_{IQE} is the internal quantum efficiency, and is described as the ratio of the photons generated inside the quantum wells (QWs) to the total number of electrons injected into the LED. This factor plays an important role in LED efficiency droop.

η_{inj} is the carrier injection efficiency to the device active region.

$$\eta_{IQE} = \frac{I_{rad}}{I} = \frac{I_{rad}}{I_{rad} + I_{lost}} \tag{1.3}$$

Total current is the sum of the current generated by the LED I_{rad} and the current lost during the process I_{lost}. Efficiency droop occurs when I_{lost} exceeds that of I_{rad}.

Carrier loss may occur inside or outside the QW, and can be accounted for the following factors as described in equation 1.4,

$$I = I_{rad} + I_{SRH} + I_{Auger} + I_{leak} \tag{1.4}$$

Non-radiative recombination processes inside the QW can either be defect-related factors such as Shockley-Read-Hall (SRH) recombination (I_{SRH}) or Auger recombination (I_{Auger}). The factors outside the QW are carrier leakage (I_{leak}).

Below, we shall further discuss these factors in some detail.

Polarization Polarization plays an important role in III-V nitride semiconductors and its performance. III-nitride semiconductors exhibit wuritze crystal structure. These hexagonal structures are defined by the edge length a, height c, and u the anion-cation bond length along the (0001) axis in units of c as shown in Figure 1.5. The Ga-N bond shows large ionicity and hence, it possesses a large piezoelectric polarization component. In addition to the large piezoelectric polarization, the III-nitride semiconductors also exhibit strong spontaneous polarization in the wuritze phase as shown in Figure 1.4.

Piezoelectric polarization is also considered as strain induced polarization which is present due to the displacement of anion sub-lattice based on interface strain. When compared to spontaneous polarization, piezoelectric polarization plays a more important role in GaN based LEDs. Spatial separation of electron and hole is caused due to the increase in polarization field leading to increase in lattice mismatch. Therefore, radiative carrier recombination efficiency is also reduced. An internal built-in electric field greatly impacts the attributes of the quantum well active regions. Since electron-hole separation is more dominant in wider wells, as compared to more narrow ones, optical gain and spontaneous emission rates are smaller in wider wells. A red-shift or a blue-shift may occur as a result of this phenomena. [21]

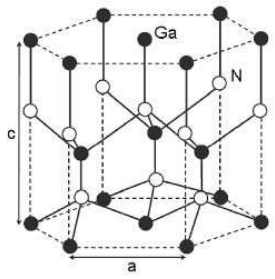

Figure 1.4 GaN wuritze crystal structure.

Crystal defects and dislocations InN and GaN have a large lattice mismatch of 11%. There are also a lack of suitable substrates for III-nitride semiconductors. Due to this, the developed LED heterostructures have very large crystalline defect densities. The dislocation density for GaN based heterostructures is typically in the range of 10^8 to 10^{10} cm^{-2}.Buffer layers, growth conditions, carrier concentration and type of impurities are factors that determine the defect formation. These defects from intermediate energy levels, and the resultant nonradiative recombination that occur at these intermediary levels are called Schockley-Read-Hall nonradiative recombination. These nonradiative recombination can have an adverse effect on the device efficiency. As described by the ABF model, parameter A is related to crystal defects and has an influence to the maximum achievable efficiency [19]. However, efficiency droop may also occur depending on the quantum well carrier density or the carrier localization related to the non-uniform indium distribution in the quantum well active regions. hence, scientists have not been able to precisely determine the role of defects in the efficiency droop if GaN-based LED, and this topic has been a subject of great interest.

Spontaneous emission Equation 1.5 shows the relation between spontaneous emission rate and carrier density,

$$\eta_{IQE} = \frac{Bn^2}{An + Bn^2} \tag{1.5}$$

It can be seen that the spontaneous emission rate depicted by η_{IQE} and is related to n as per equation 1.5. This holds true for low injection currents. However, at high injection currents, it shows a non-linear dependency on n. [24] Using this relation, the following graph in Figure 1.5 has been plotted to show this dependency.

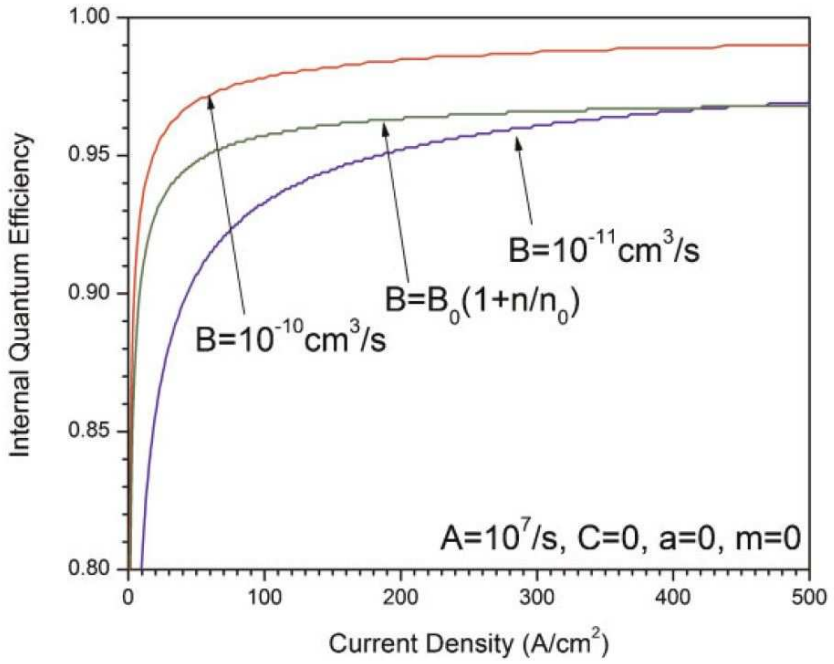

Figure 1.5 Influence of the radiative recombination coefficient, B , on the IQE.

The resulting IQE values are compared to the cases with constant B parameters. This relationship does not directly affect efficiency droop but lowers the barrier for the non-radiative process to trigger the efficiency reduction.

Auger Recombination During the non-radiative electron-hole recombination process, there is production of excess energy. This excess energy is utilized by electrons and holes in the same energy band and are then excited to higher bands themselves. This is the Auger recombination process. Auger coefficient C is used to describe the probability of the Auger recombination process. Wide bandgap semiconductors generally exhibit a smaller Auger recombination rate, compared to semiconductors with a narrower bandgap. For GaN (3.4 eV), the expected

Auger coefficient C is $10^{-34} cm^6 s^{-1}$[23]. However, much lower values (in the range of $10^{-30} cm^6 s^{-1}$) have been reported for InGaN alloys [39] [18] [14]. With these values, 13 efficiency droop can be explained [24] even we when assume that the carrier leakage is nearly zero in the ABF model with A and B values being 107 s^{-1} and $2 \times 10^{-11} cm^3 s^{-1}$ Inhomogeneous Carrier Distribution, respectively. Evidently, efficiency droop increases as the Auger coefficient C becomes larger.

In-homogeneous carrier distribution Holes, by nature have high effective mass and low mobility. Due to this, the hole mobility in LED active regions may be inefficient. Therefore, injected holes are majorly located close to the p-doped GaN layer and this concentration tapers off as it approaches the n-type side. On the contrary, electrons have a more uniform carrier distribution throughout the device. This leads to highly inhomogeneous carrier distribution throughout the LED device active regions. The hole density reduces steeply from p-GaN to n-GaN, resulting in non-uniform hole distribution in the MQWs. This issue can be tackled by reducing the thickness of the barrier thickness. This would allow hole injection to occur more freely, therefore, reducing electron leakage. This would also lead to significantly augmented Auger recombination and increase in electron overflow, further limiting the optical emission efficiency at high injection levels. P-doped active region and thin InGaN barrier have been used as solutions to improve the performance of conventional InGaN/GaN QWs.

Electron overflow The above factors involve internal factors that effect efficiency. Electron overflow is however an external phenomena and can result because of numerous possible situations. The band energy tilts because of the polarization fields, reducing carrier recombination. Nonuniform carrier concentration can also cause a polarization field to occur which leads to electron leakage out of the LED active region, which can recombine with holes in the p-GaN region therefore they can reach

the active region. Reduction in energy barrier due to the built-in polarization field is one of the main reasons for electron overflow. The presence of a polarization field causes the band gap to be tilted downward near the p-GaN region. This problem generally occurs in Ga-polar III-nitride LEDs. To tackle this issue, an electron beam layer (EBL) is utilized, often made up of AlGaN dude to its high band gap. However, an EBL cannot completely nullify electron overflow, and efficiency droop can still occur.

1.5 Motivations of Using III-nitride Materials

There is much current interest in the optical properties of semiconductor nanowires, because of the strong two-dimensional confinement of electrons, holes and photons make them particularly attractive as potential building blocks for nanoscale electronics and optoelectronic devices including lasers and nonlinear optical frequency converters. Gallium nitride (GaN) is a wide-band gap semiconductor of much practical interest, because it is widely used in electrically pumped ultravioletblue LEDs, lasers and photodetectors. [11]

III-nitride materials used in our nanowire LED structures have a direct band gap and a high band gap tunability due to effective strain-relaxation, hence we can use this material structure to generate light in wide range of wavelengths varying from UV to IR. This ability to engineer the band gap of our device allows to create LEDs of a full range of colors including red, orange, yellow, green, blue, UV and even white colors [21]. This has enabled us to demonstrate white LEDs without phosphor films involved [22].

GaN and its low dimensional structures have been extensively investigated in the past years due to their excellent optical and electrical properties. Progress in this field is so fast that the nitrides are expected to revolutionize the optoelectronics and electronics in the new century. The nature of high thermal conductivity, high

luminous efficiency and mechanical robustness have made GaN and its alloys the superior material system for light emitting devices operated from the UV to the entire visible spectra region. In addition, new applications in high power, high temperature and high frequency electronic devices based on GaN field effect transistors and heterobipolar transistors is under extensive exploration.

Compared to their conventional planar counterparts, III-nitride nanowires can be largely free of dislocations and piezoelectric polarization field, due to the effective lateral strain relaxation associated with the large surface-to-bulk-volume ratio. In addition, recent studies have shown that nearly defect-free III-nitride nanowires can be grown virtually on any substrates. Moreover, due to their significantly reduced dimensions, III-nitride nanowires offer a new avenue to scale down the dimensions of future devices and systems. In the past decade, a broad range of III-nitride nanowire optoelectronic devices have been demonstrated, including LEDs [35], lasers [2], photodetectors [8] and solar cells [36] among many others.

1.6 Thesis Preview

In this thesis, we have first performed detailed study on the design of nanowire LEDs, then the MBE growth, fabrication and characterization of superior quality InGaN/AlGaN nanowire LEDs on Si(111) and copper substrates. Full-color LEDs operating in the visible wavelength regime was investigated, followed by the development of UV-B LEDs. The flow of this thesis is described below.

Chapter 1 presents general information related to our research including nanowires, III-nitride nanowire and loss mechanism in LEDs. Chapter 2 describes the design procedure, fabrication process and a preview of the methods we use to fabricate our devices. Chapter 3 is a discussion of visible nanowire LEDs and what the various parameters that we have found that affects the performance of these nanowires. Chapter 4 talks about the device performance of LED nanowires in the

UV-B range of spectra. Chapter 5 is a discussion on the future studies we aim to eventually conduct in this sphere of research.

CHAPTER 2

DESIGN, FABRICATION AND CHARACTERIZATION METHOD

2.1 Design

The first and foremost step in our efforts to fabricate novel nanowire LEDs with high output power and reduced efficiency droop. Therefore, the device structure is carefully designed. Some major factors have been seriously concerned during the device design phase, listed below:

- Which wavelength do we want the structure to emit? The wavelength of the light emitted is a critical piece of information which we use to design our nanowires. Depending on the wavelength, the material used changes, the dimensions of the nanowires themselves changes, and details like which substrate would be suitable for growth purposes and would we need metal contacts to aid the conductivity of electrons through the device.

- Is the structure feasible to fabricate? (fabrication has limitations, designing does not) All ideas for the design of the most effective nanowire cannot be practically implemented due to limitations in fabrication. Limitations in fabrication can be accounted to limits to which the equipment we have. For example, we cannot obtain a nanowire array with a radius of 10 nm due to limited growth conditions including temperature and In/Ga flux ratios. Moreover, we have to account for the randomness in fabrication, such as a nanowire with radius of 50 nm may actually have a radius of 45 to 55 nm. This will definitely affect the performance of the device.

- What are we trying to achieve out of the structure? The main objective of using nanowire structures is to serve as some sort of practically usable device. This may be an LED (light output), LASER (lasing action), photodetector, solar cell

etc. Each of these devices has different optoelectronic phenomena which would result in the desired action. Hence, the device structure for each application is varied and need to be designed to suit for its applications.

- What is the overall LEE of the device? LEE is an important factor while designing the nanowire LED structure. After the basic nanowire design is completed, we run a set of simulations (will be described further in this chapter) to obtain the structure which has the highest LEE. Since the simulation is done by computers, we may get values which are not possible to fabricate in labs, and hence decide on dimensions which are as close as possible to the optimized results.

- Why a certain existing structure is behaving in a particular way and what can we do to improve it? There has been a great deal of research and development in the field of nanowire design. The numerous groups in the world are all working on what the best structure is for a specific design, and as we progressively better our understanding of these quantum structures, the more we learn on how to improve. Hence, a large portion of our efforts is rested in improving previous models by trying to reason why they performed the way they did.

The process of design begins with the simulation software that we use called, FDTD (finite difference time domain) Lumerical. This software package offers ability to replicate conditions that would closely resemble the performance of the fabricated LED device. Therefore, the device fabrication and results are close to what we expected since they were facilitated by the properly designed structures with favorable parameters. There are standardized methods for the determination of material parameters to assess the relationship between the properties of the grown material, the device structure and the device performance. Externally emitted power is usually the parameter used for device performance, P_{out}. From here on out, two other quantities

determine LED performance; the wall plug efficiency (WPE), η_{wpe} i.e., the ratio of electrical input power to optical output power, and the external quantum efficiency (EQE), η_{EQE} , the ratio of number of electrically injected carriers and externally observed photons.

WPE and EQE are related to each other through the diode forward voltage and series resistance, as,

$$\eta_{wpe} = \frac{P_{out}}{VI} \tag{2.1}$$

Where I is the injected current, V is the voltage across the device, and P_{out} is the light output.

To achieve a high value of EQE, structures with high conductivity materials and low resistance contacts are required.

The EQE is the product of IQE and the LEE, η_{extr} of the material. The IQE is the ratio of the electrically injected carriers and the internally emitted photons, which in itself is the product of the electron injection efficiency η_{inj}, ratio of carriers reaching the light emitting region, which in our case are the MQW to those injected in the device and of the radiative efficiency, η_{rad}, ratio of injected electron-hole pairs that recombine in a radiative manner to generate photons to the total number of injected electron hole pairs. The LED heterostructure mostly determines the η_{inj}. η_{extr} can be optimized through various techniques such as photonic crystals (which we will use, chip shaping, use of patterned substrates), surface roughening etc.

The structure design is the major factor for η_{rad} (choice of material compositions and layer thickness) and for a given structure by the materials quality linked to growth conditions (temperature, pressure, precursor flux and unintentional impurity incorporation) affecting the crystal quality.

The above terms can be mathematically related in the following manner

$$P_{out} = (\frac{\hbar\omega}{q}) I \eta_{inj} \eta_{rad} \eta_{extr} \tag{2.2}$$

$$\eta_{EQE} = \eta_{inj} \eta_{rad} \tag{2.3}$$

where $\hbar\omega$ is the photon energy and q is the electron charge.

We shall now discuss about η_{extr} or in other words, LEE. Since we are giving such importance to this parameter, it would be beneficial to understand the physics behind it's significance. Photons are generated in the active region of our structure and they propagate throughout the material. majority of the generated photons are totally internally reflected back into the structure but a small fraction does escape into the surroundings. The emitted photons then reattempt to escape the LED numerous times (eventually being extracted by bouncing back within the light cone at an exposed surface), to be either reabsorbed by active material and dissipated by material defects and free carriers in doped regions or metallic materials.In the former case, the photons are re-emitted by the active region and reattempt to escape the LED giving rise to an effectively increased LEE. This is called photon recycling and is shown in Figure 2.1.

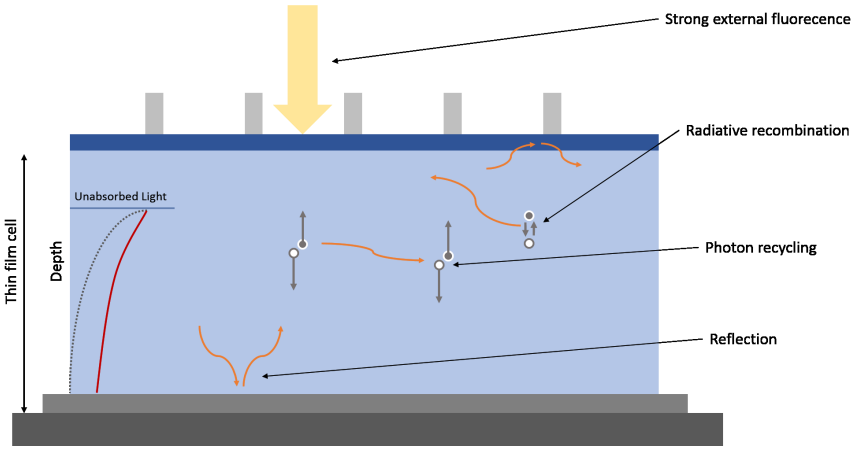

Figure 2.1 Illustration of the photon recycling process.

The emitted photons can escape which makes quantifying LEE accurately a difficult task. This majorly depends on the design of the LED device. The LEE based on the based on the use of features like truncated pyramids, roughened surfaces, patterned sapphire substrates, and surface photonic crystals is difficult to quantify and much depends on the geometry of the LED device. Hence, we use finite difference time domain analysis, which runs Maxwells equations to replicate the above scenario and come to an scientifically agreeable value of LEE.

2.1.1 Nanowire Light-emitting Diodes and Light Extraction Efficiency

Properties like dimension, spacing, radius etc. are important design parameters to the overall light extraction efficiency. Understanding how these physical factors affect the output is fundamental to an effective design.

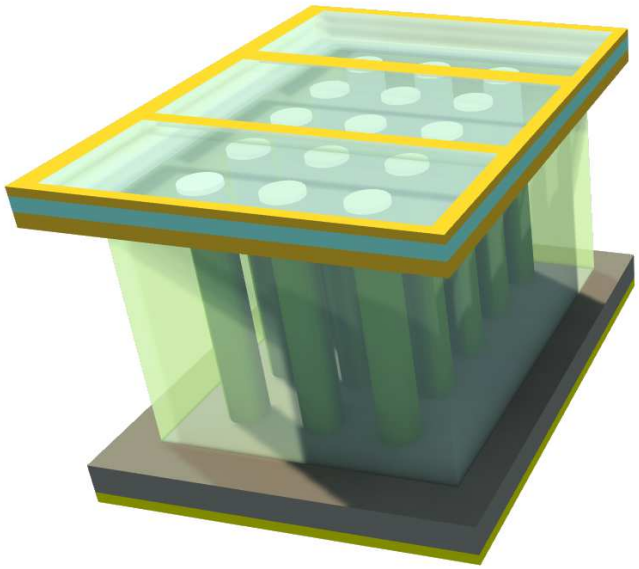

Figure 2.2 3-D model of nanowire LED device with metal contacts.

Figure 2.2 shows a schematic structure of the nanowire LED device. The nanowires here, are arranged in a hexagonal array (abab). There are other methods of arranging the nanowires, such as square (aaaa) or in a circular fashion. However, the use of the hexagonal arrangement is widely accepted, both due to ease of design

and fabrication. These different structures are shown to demonstrate many methods one can design a nanowire structure based on the same materials and dimensions. We have merely rearranged the various segments of the nanowire and as we will observe, the performance changes quite dramatically.

2.1.2 Simulation

Personally, I have had the most exposure in my term in the research group with this phase, hence it is most rewarding when the fabricated device results come in, as we can directly compare it to the results in our design phase. Comparing calculated predictions with actual results, which scientist (budding) does not love a challenge like that.

We use a software called, FDTD Lumerical for our simulation procedure. FDTD is perhaps the simplest of the full-wave techniques used to solve problems in electromagnetics. FDTD is a numerical analysis technique used for modeling computational electrodynamics (finding approximate solutions to the associated system of differential equations). It is a time-domain method and thus, the solutions can cover a wide frequency range with a single simulation run, and treat nonlinear material properties in a natural way. This method loosely fits into the category of resonance region methods, i.e., ones in which the characteristic dimensions of the domain of interest is in the order of a wavelength in size. If the dimensions of the object are not in the range, then other methods such as quasi-static approximations and ray-based among other techniques are used. [1]

How does FDTD work? In this section, we will be discussing how a FDTD solution works. The FDTD method employs finite differences as approximations to both the spatial and temporal derivatives that appear in Maxwells equations (specifically Amperes and Faradays laws). The derived finite-difference equations are then solved in a leapfrog style, i.e., the electric field vector components in a

volume of space are solved at a given instant in time; then the magnetic field vector components in the same spatial volume are solved at the next instant in time; and the process is repeated over and over again until the desired transient or steady-state electromagnetic field behavior is fully evolved.

To portray a simpler image, it is making movies of the field (electromagnetic) where each frame is one iteration of the loop mentioned above. Below is a simplified algorithm, [1]

- Set all fields to zero
- Update electric field by calculating curl of magnetic field
- Add to current value of electric field
- Update magnetic field by calculating curl of electric field
- Add to current value of magnetic field
- Update sources (electric field source and magnetic field source) after each iteration
- If there are any materials in the field, it will change the values of the field
- Handle electric and magnetic field boundaries
- Record simulation data
- Show simulation status
- If there are various materials with different optical values, we derive D from H and E from D (D = absalon * E)
- Similarly for H, we get from E which we get from B (B = mew * H)

- This way we accommodate different materials in our simulation and their interaction with the source

Like any other method, FDTD has its strengths and weaknesses. Strengths

- FDTD is a versatile modeling technique used to solve Maxwell's equations. It is intuitive, so users can easily understand how to use it and know what to expect from a given model.

- FDTD is a time-domain technique, and when a broadband pulse (such as a Gaussian pulse) is used as the source, then the response of the system over a wide range of frequencies can be obtained with a single simulation. This is useful in applications where resonant frequencies are not exactly known, or anytime that a broadband result is desired.

- Since FDTD calculates the E and H fields everywhere in the computational domain as they evolve in time, it lends itself to providing animated displays of the electromagnetic field movement through the model. This type of display is useful in understanding what is going on in the model, and to help ensure that the model is working correctly.

- The FDTD technique allows the user to specify the material at all points within the computational domain. A wide variety of linear and nonlinear dielectric and magnetic materials can be naturally and easily modeled.

- FDTD allows the effects of apertures to be determined directly. Shielding effects can be found, and the fields both inside and outside a structure can be found directly or indirectly.

Weaknesses

- Since FDTD requires that the entire computational domain be gridded, and the grid spatial discretization must be sufficiently fine to resolve both the smallest

electromagnetic wavelength and the smallest geometrical feature in the model, very large computational domains can be developed, which results in very long solution times.

- Models with long, thin features, (like wires) are difficult to model in FDTD because of the excessively large computational domain required
- There is no way to determine unique values for permittivity and permeability at a material interface.
- Space and time steps must satisfy the CFL condition, or the leapfrog integration used to solve the partial differential equation is likely to become unstable.
- FDTD finds the E/H fields directly everywhere in the computational domain. If the field values at some distance are desired, it is likely that this distance will force the computational domain to be excessively large. Far-field extensions are available for FDTD, but require some amount of post processing.[4]

We generally run simulations for one particular wavelength, specific radius and spacing of nanowire array. To visualize a nanowire array for the sake of explanation, I have demonstrated a Figure 2.3 which shows a typical nanowire array and its various segments.

Process In this section, we will discuss what the process of running a simulation on FDTD Lumerical in our research group is. Figure 2.3 which shows the start up screen in FDTD Lumerical. Within the four panes of observation (perspective from different combination of any 2 axes), a nanowire array structure has been designed. To explain the process of running a simulation, I will use this image to express the various virtual tools we use to replicate a near real time scenario. The following figures, Figures 2.3 and 2.4 illustrate these mentioned parts of the software.

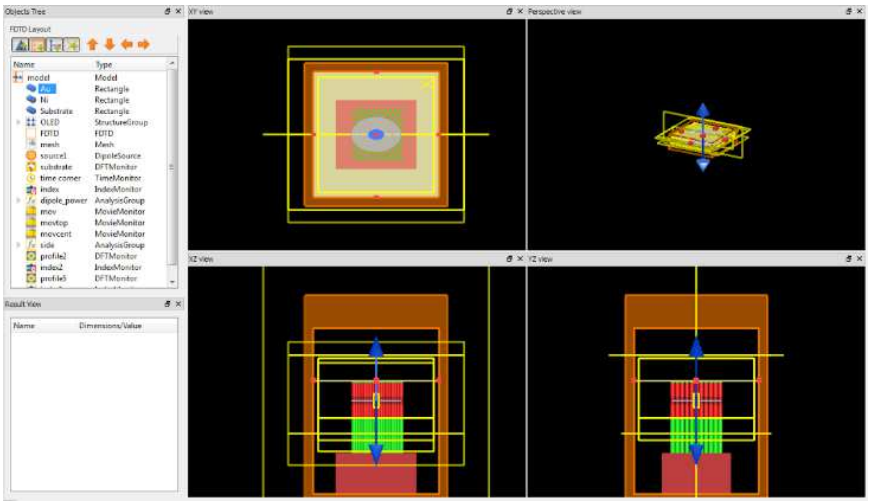

Figure 2.3 An example of a typical Lumerical Layout for the purpose of design and simulation.

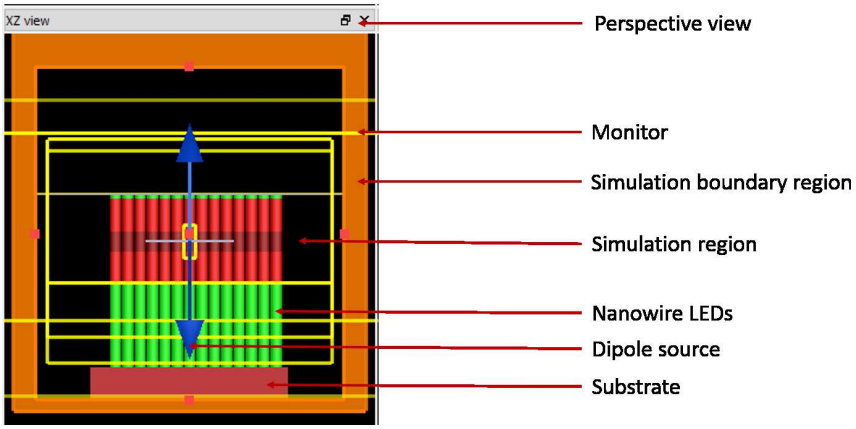

Figure 2.4 An inset of the Lumerical Layout for design purposes showing individual components.

Here we can see that the each nanowire is constructed in layers as defined in Figure 2.4. The materials we use, their respective composition and dimensions all determine how the nanostructure will behave. The software has an existing database of different materials and the refractive index (real and imaginary) at various wavelengths. The user can add new custom materials referred from values which are scientifically agreeable. Each material has it's own color for visual differentiation. Using the shaping tools in the software, the user is able to create an array of nanowires with identical dimensions and constitution. The array itself has properties of radius and spacing which we vary to acquire the greatest value of light extraction efficiency; this process is called optimization of the nanowire array. Depending on the design of the structure, we may require either a silicon based substrate or a metallic substrate. The orange box surrounding the nanowire array is the border for the simulation region, within which the software will run the FDTD based equations. The various yellow lines around the nanowire array are monitors. Monitors are tools which receive information based on the mathematical equations running within the simulation region, and store data which we can later on extract. Hence, monitors are effectively the senses of the software and the general rule of the thumb is, the more monitors that are used, more beneficial it is. We generally place monitors on all sides of the array, and a few within the array. This gives us an idea as to how the light energy is propagating and reacting within the nanowire array. Below we can see some of the output data from electric field monitors that were placed in the nanowire array as seen is Figure 2.4.

Figures 2.5 and 2.6 show the output of these monitors we use after a simulation of a model is complete. This helps us in numerous ways, for example using the following figures, we can observe how the electric field is distributed across the nanowire array and around it.

Monitors themselves have various types.

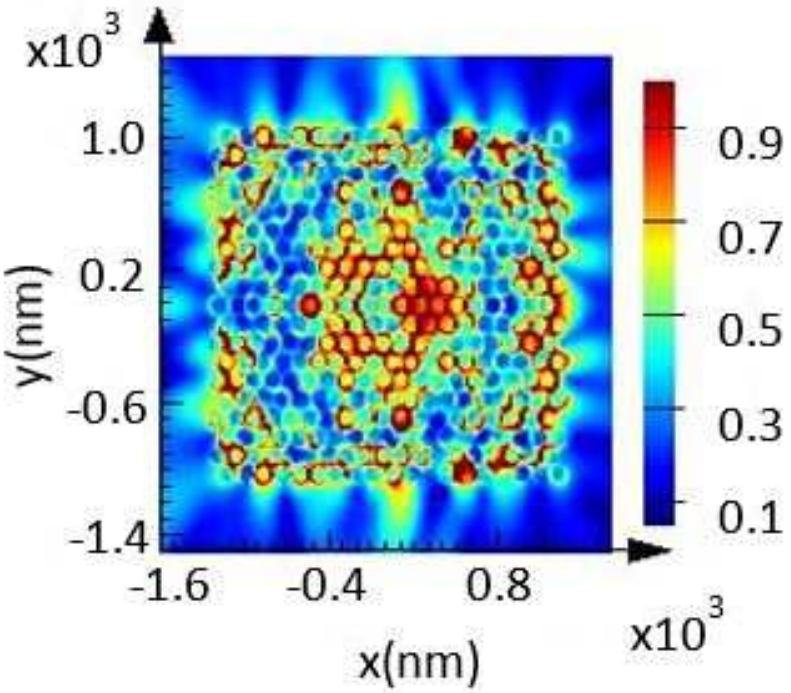

Figure 2.5 An example of electric field distribution of a nanowire array.

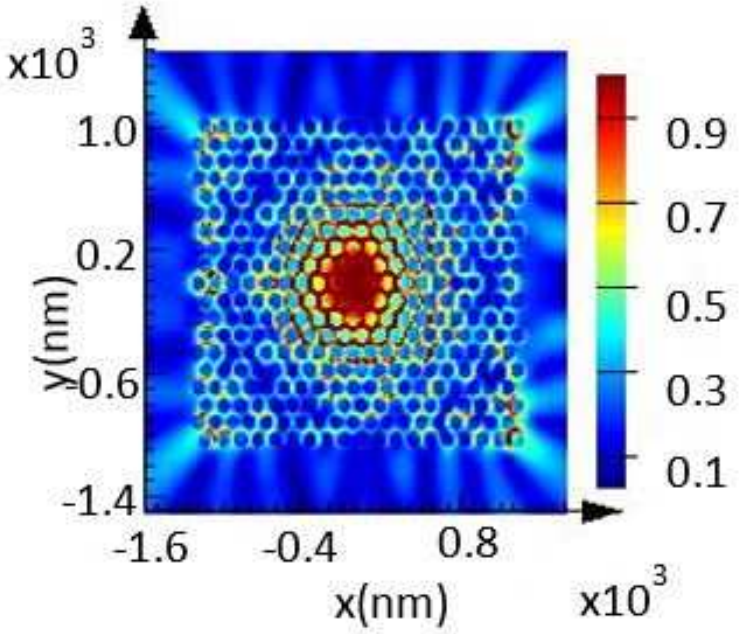

Figure 2.6 An example of electric field distribution of a nanowire array.

- Refractive index
- Field time
- Movie
- Frequency Domain Field Profile
- Frequency Domain Field and Power
- Mode expansion

We regularly use Frequency Domain Field and Power monitor. This monitor gives us extensive data on output electric field (in all 3 axes), output magnetic field (all 3 axes), output power (all 3 axes), light extraction efficiency and far field data (electric field at a distance). With this data, we can decide if the structure should be used for fabrication purposes.

Another monitor which is very helpful for visual purposes is the movie monitor. The movie monitor uses the above mentioned FDTD algorithm to create a video which we can playback and observe how the electric field is propagating throughout the array. This is helpful not just for visual purposes, but it shows us how various materials behave with that frequency of light. For example, if the material is very absorptive at a particular frequency, the output parameters like LEE and power would be low and the video representation would confirm that the light has indeed been absorbed by the material as less of it is seen to be propagating out of the array. This monitor is especially helpful for a less experienced student or scientist to understand how light behaves with variation of material and dimensions of the structure.

The next important tool is the source. The source, like the monitor has various types:

- Dipole

- Gaussian
- Plane Wave
- Total field scattered field
- Mode
- Import

We use the dipole source in most of our simulations. This resembles the practical scenario and accurate results have been verified in previous experiments. [7] We use the other types of sources for other situations.

This is the fundamental of FDTD Luemrical design and more on this software can be found on their website. https://www.lumerical.com/tcad-products/fdtd/

2.2 Fabrication of Nanowire Light-emitting Diodes

Currently, two most popular methods of growing III-nitride nanowires are MOCVD and MBE. MOCVD has been used to produce optoelectronic devices on a large scale, which has led to commercial production of LEDs and LDs. MBE however, due to the lack of efficient nitrogen sources to aid the growth process, has not been able to produce on a large scale. The advantages of using an MBE system over MOCVD are for example, better interface control and the suitability for exploring new material structures or achieving high quality crystalline materials, it can provide the highest control of the epitaxial growth of various nanostructures, ultra-high vacuum environment ($1 \times 10^{-10} Torr$) and a slow deposition rate (typically less than 1000 nm/hr), which is useful to minimize impurity incorporation in the epitaxial layers and the MBE growth temperature is also much lower than that of MOCVD, which can enhance indium incorporation, leading to the realization of high indium content InGaN structures. Moreover, by using the MBE growth technique, the composition and thickness of the epilayer can be controlled precisely to mono-atomic layer level.

Its in-situ monitoring capability can also greatly assist researchers to manage the growth quality and to develop new materials.

The MBE growth process of III-nitride structures can be divided into two categories, based on the nitrogen sources, including ammonia-molecular beam epitaxy (Am-MBE) and plasma-assisted molecular beam epitaxy (PAMBE), respectively. We have utilized the PAMBE method to produce our devices. in the case of PAMBE, a plasma source of high purity inert N2 gas is used to supply the group V element. The active nitrogen plasma includes ionized molecules (N_2^+), atoms (N), and ionized atoms (N^+). In this thesis, III-nitride nanowire heterostructures were grown by a Veeco Gen II MBE system equipped with a RF plasma-assisted nitrogen source. Figure 2.7 shows the MBE system in the NanoOptoelectronics Laboratory in the Department of Electrical and Computer Engineering. The MBE system consists of three main vacuum chambers including an intro-chamber, a buffer chamber, and a growth chamber. Si substrates are first cleaned by standard cleaning techniques such as hydrogen fluoride (HF) acid treatment or RCA, which are introduced into the chamber for the In(Ga)N deposition. The amount of active nitrogen plasma can be well controlled by adjusting the nitrogen flow rate and the plasma power (the maximum power is generally at 500 W).

In this thesis we have used the Veeco Gen II MBE system equipped with RF plasma-assisted nitrogen source. Figure 2.7 shows the above mentioned system in the New Jersey Institute of Technology Electrical and Computer Engineering Department.

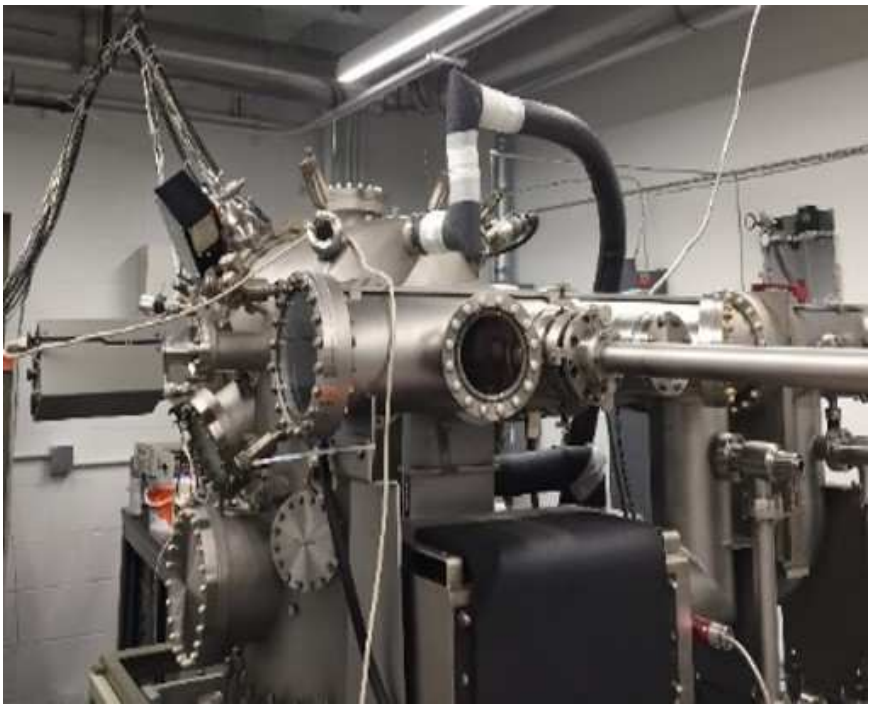

Figure 2.7 Molecular beam epitaxy system in the NanoOptoelectronics Laboratory.

2.3 Characterization Methods

In this section we study the methods used to analyze the device we have designed and fabricated. Analysis here refers to finding the output wavelength of emission, stability of emitted light and the devices diode characteristics.

2.3.1 Electroluminescence

Electroluminescence (EL) characterization is used to analyze the spectrum of light which the nanowire LED devices produce. This is essential to confirming that our design parameters and fabrication has manufactured a device which is in accordance to our expectations. To measure the EL graph, we use a probe, which senses the biased nanowire LED device and plots it in a graph using the software Spectra Suite.The LED nanowire device is biased by power supply (using either voltage source or current source). The EL graphs also help us measure the performance of the LED device, in particular, the blue or red shift. This shift is an unfavorable phenomena, and can

easily be observed from overlapping EL graphs at varied intensities. Figure 2.8 shows a sample EL spectra collected from a visible nanowire LED.

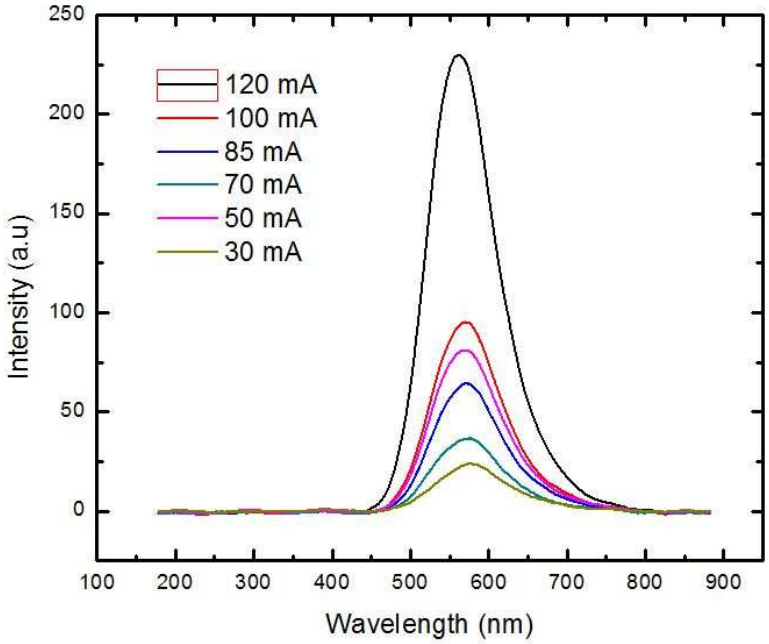

Figure 2.8 Electroluminescence spectra of visible LED under different injection currents.

2.3.2 Photoluminescence

Photoluminescence(PL) spectroscopy is a method in which the electronic structure of material is exposed to a direct source of light. The material absorbs this light and is imparted with excess energy. One way it can dissipate this excess energy is through the emission of light, or luminescence. In the case of photo-excitation, this luminescence is called photoluminescence. In our study, PL spectra of the nanowire LEDs were measured using 405 and 266 nm lasers as the excitation source at room-temperature. The photoluminescence emission was collected by a microscope objective, spectrally resolved by a high-resolution spectrometer, and detected by a photomultiplier tube. PL graphs can be conducted at various temperatures to observe

the effect of temperature on the performance of the device. Figure 2.9 is a sample PL v/s wavelength graph at 300 K.

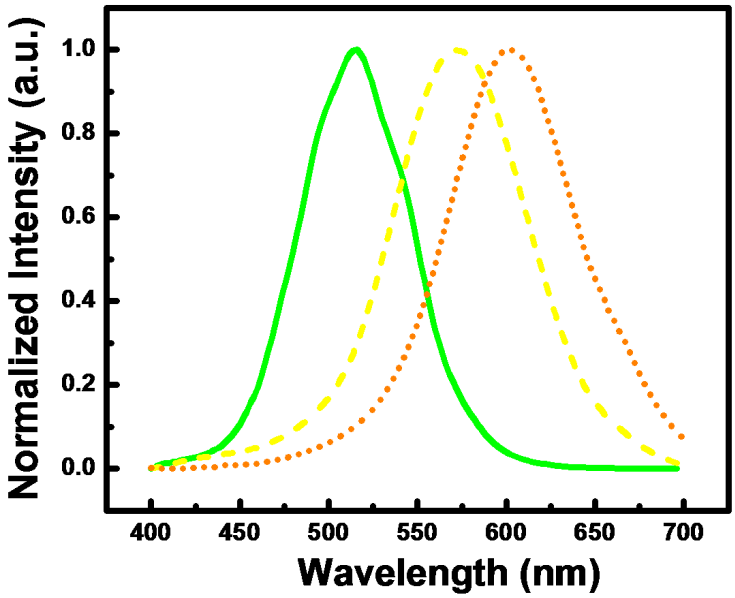

Figure 2.9 Photoluminescence versus wavelength graph.

2.3.3 Current-voltage Characterization

Current versus voltage (I-V) characteristic is useful to determine the diode properties of the fabricated device. We can calculate the turn on voltage, shunt resistance, series resistance, and power by integrating the graph and acquiring the area under curve. Below is an example of an I-V curve in Figure 2.10.

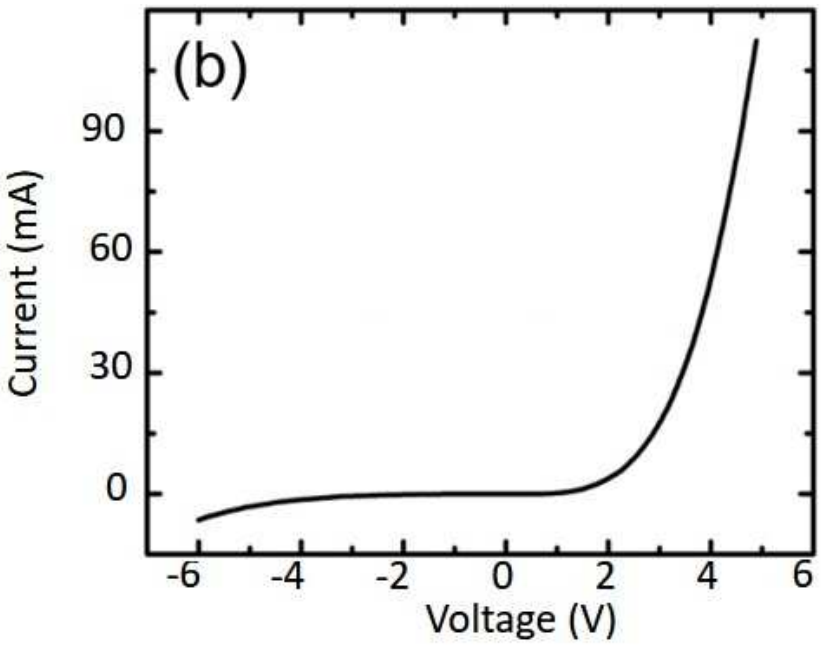

Figure 2.10 Current-voltage characteristic of an InGaN/AlGaN nanowire LED.

CHAPTER 3

VISIBLE NANOWIRE LIGHT-EMITTING DIODES

3.1 Introduction

In this chapter, we report on the achievement of full-color nanowire LEDs and, our study on high performance nanowire LEDs on copper (Cu) substrates via substrate-transfer process.

This chapter will broadly be divided in two sections. The first part describing color tunable nanowire LEDs fabricated by MBE, and the second part describing our study on high performance nanowire LEDs on Cu substrate.

3.2 Full-color Nanowire Light-emitting Diodes Grown on Silicon

We report our study on full-color nanowire LEDs, with the incorporation of InGaN/AlGaN nanowire heterostructures grown directly on the Si (111) substrates by MBE. Multiple color emission across nearly the entire visible wavelength range can be realized by varying the In composition in the InGaN quantum dot active region. Moreover, multiple AlGaN shell layers as seen in Figure 3.1, are spontaneously formed during the growth of InGaN/AlGaN quantum dots, leading to the drastically reduced nonradiative surface recombination, and enhanced carrier injection efficiency. Such core-shell nanowire structures exhibit significantly increased carrier lifetime and massively enhanced photoluminescence intensity compared to conventional InGaN/GaN nanowire LEDs. A high color rendering index of around 98 was recorded for white-light emitted from such phosphor-free core-shell nanowire LEDs.

3.2.1 Device Fabrication

The device fabrication route of InGaN/AlGaN dot-in-a-wire core-shell devices comprises of the following steps. After the nanowire array are grown by MBE,

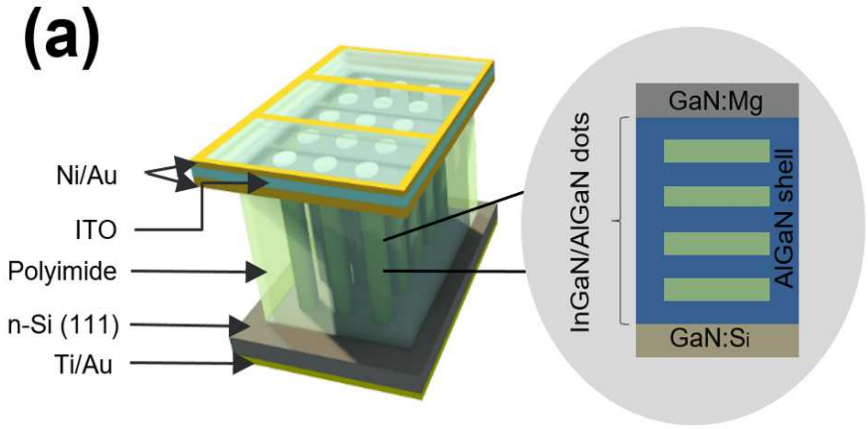

Figure 3.1 Schematic illustration of an InGaN/AlGaN dot-in-a-wire core-shell LED heterostructure on Si substrate. The inset depicts the layer by layer structure.

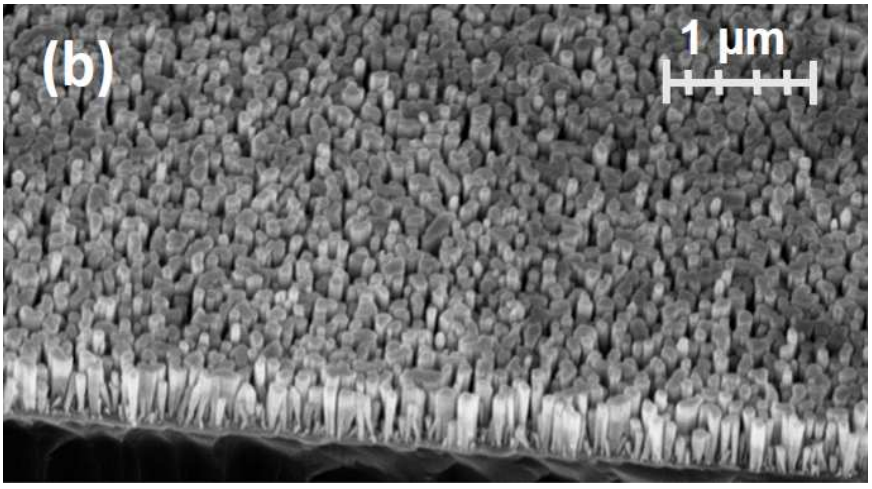

Figure 3.2 A 45 degree tilted SEM image of a typical InGaN/AlGaN core-shell nanowire LED sample.

they were spin-coated with polyimide resist for planarization and passivation, which is followed by O2 dry etching to expose the top region of the nanowires. The exposed GaN:Mg surface were then deposited with layers including Ni (5 nm)/Au(5 nm)/indium tin oxide (ITO) to form top metal contacts. Afterwards to form the backside and topside contacts respectively, Ti/Au (10 nm/100 nm) and Ni/Au (10 nm/100 nm) layers were evaporated on the backside of the Si substrate and top of ITO respectively. Additional information regarding the MBE growth and device fabrication of such nanowire LEDs can be found elsewhere [22] [24] [20]. The schematic of this structure can be found in Figure 3.1 and a SEM image of a sample in Figure 3.2.

3.2.2 Results and Discussion

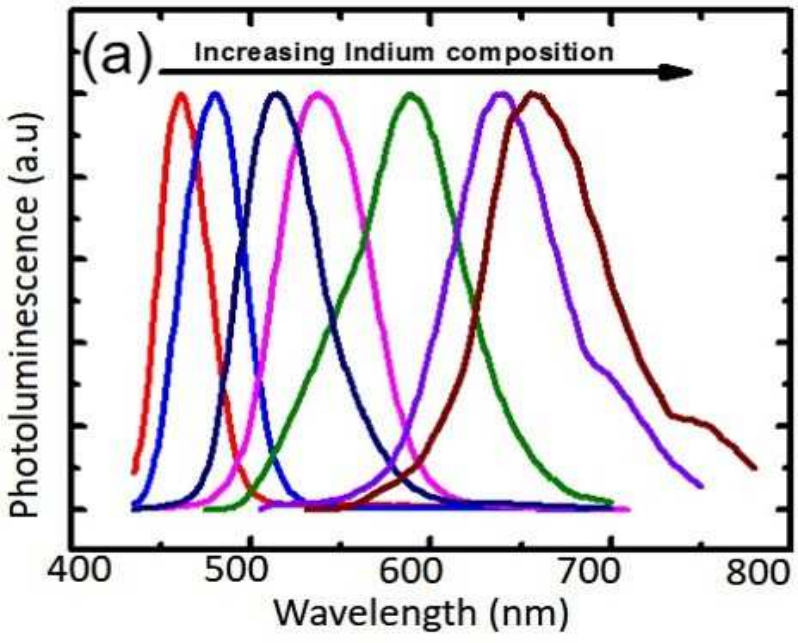

Figure 3.3 Normalized room temperature photoluminescence spectra of multiple emission colors from multiple InGaN/AlGaN nanowire LEDs.

Optical properties of InGaN/AlGaN dot-in-a-wire LED heterostructures were investigated by using PL spectroscopy with a 405 nm laser as an excitation source at

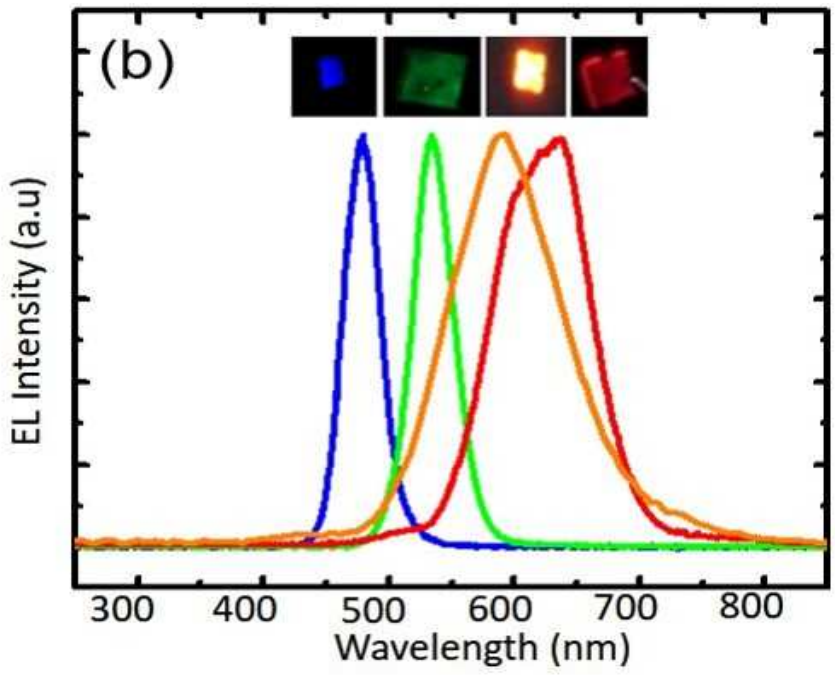

Figure 3.4 Electroluminescence spectra of various InGaN/AlGaN LEDs with distinct emission colors, along with their optical image.

room temperature as shown in Figure 3.3. Full-color emission with wavelengths can be readily tuned across nearly the entire visible wavelength range. Shown in Figure 3.4, the peak emission wavelength of InGaN/AlGaN core-shell nanowire LEDs varies from 460 nm to 660 nm. Effective variation in the In composition in the InGaN quantum dots can be achieved either by using different growth temperatures and/or In/Ga flux ratios. A longer wavelength as in red light is typically associated with a lower bandgap material. This gives us an impression about the composition of In in the nanostructure to achieve the desired color of light from the active region. The above suggests that in the room temperature PL spectra, In composition increases from a lower value to a higher value for switching from blue to red color emission in the visible spectrum. The latter engineered structures can be used to envision different color emissions as expected.

3.3 High Performance Nanowire Light-emitting Diodes on Copper

We report our study on the development of high performance nanowire LEDs on Cu substrates via substrate-transfer process. Nanowire LED structures were first grown on silicon-on-insulator (SOI) substrate by MBE. Subsequently, Si substrate was removed by combining dry and wet etching processes. Compared to conventional nanowire LEDs on Si, nanowire LEDs on Cu exhibit several advantages, including more efficient thermal management and enhanced light extraction efficiency due to the usage of metal-reflector and highly thermally conductive metal substrates. The LED on Cu, therefore, has stronger photoluminescence, electroluminescence intensities and better current-voltage characteristics compared to conventional nanowire LED on Si. Our simulation results further confirm the improved device performance of LED on copper, compared to LED on Si. The light extraction efficiency of nanowire LED on Cu shows 9 times higher than that of LED on Si at the same nanowire radius of 55 nm and spacing of 130 nm. Moreover, by engineering the device active region, we achieved high brightness phosphor-free LEDs on Cu with highly stable white light emission and high color rendering index of greater than 95, making it a promising candidate for potential applications in general lighting, flexible displays and wearable applications.

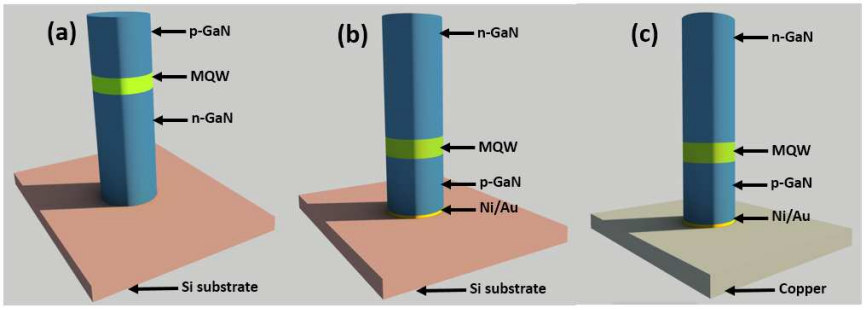

Figure 3.5 Comparison of 3 types of nanowire LED design.

Illustrated in Figure 3.5, three InGaN/AlGaN nanowire LED structures were comprehensively studied utilizing finite 'difference time domain (FDTD). These LED

structures include conventional p-side up nanowire LED on Si substrate (LED1), n-side up LED on Si substrate (LED2), and n-side up LED on metal substrate (LED3), shown in Figures 3.5(a), (b), and (c), respectively. N-side up LEDs can also be called as flip-chip LEDs throughout this paper. The device structure is composed of an n-GaN layer, InGaN/AlGaN multiple quantum well active region and a p-GaN layer. The active region is composed of ten InGaN wells (3 nm thick layer) sandwiched by 3 nm AlGaN barrier layers. The thickness of the n- and p- type regions are 350 nm and 150 nm, respectively. The underlying substrate is assumed to be Si ($300nm$) and metal for the typical and flip-chip InGaN/GaN nanowire LEDs, respectively. The refractive indices are shown in the Table 3.1.

Table 3.1 Refractive Index of Materials used.

	Material	*Refractive index*
(i)	n-GaN	2.7
(ii)	MQW	2.6
(iii)	p-GaN	2.7

Lumerical FDTD solution is employed to numerically investigate and compare LEE of nanowire LEDs versus spacing and radius of nanowires. The measuring monitors are placed above the LEDs to collect all optical power emitting from the designed nanowire device structures. The nanowire LEDs grown by MBE have radius in the range of 40 to 80 nm. In our simulation, therefore, we first considered the nanowire array with hexagonal arrangement of 50 nm radius and spacing between the centers of the nanowires is 130 nm, and device area is $2.5 \times 2.5\mu m^2$ for all LED devices. The geometry of the nanowires has a dominant effect in the emission of generated photons from active region into air. The radius and spacing of nanowires

are among the parameters which can be used to maximize the LEE of nanowire LEDs. With proper design of nanowire spacing and radius, the light can be coupled through nanowires and scattered out of the device.

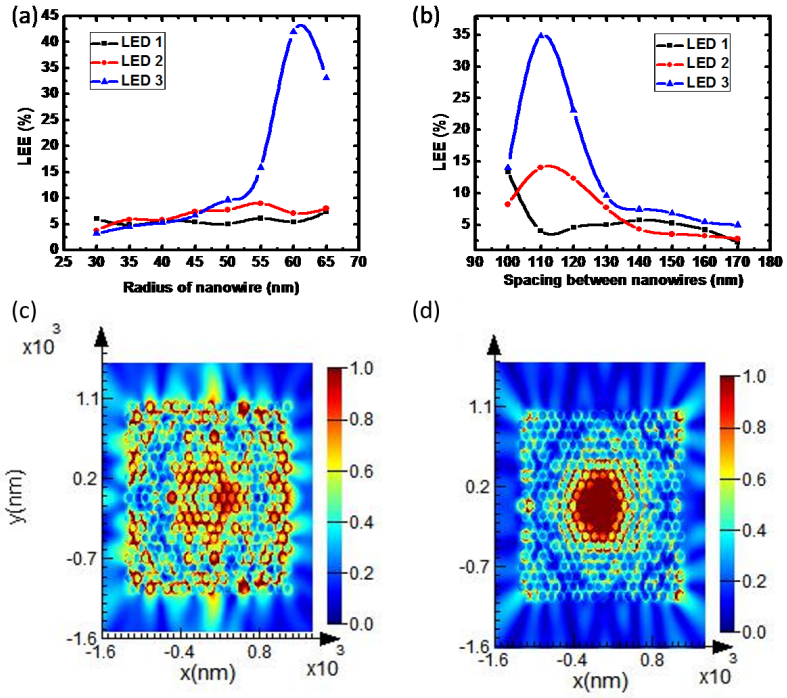

Figure 3.6 (a). Variation of LEE with change in spacing (for a constant radius of 50 nm) and (b) change in radius (constant spacing of 130 nm) for the flip chip structure (n-i-p) on metal and normal (p-i-n) structure on substrate. (c) Electric field distribution plot from top monitor for a flip chip on metal and (d) Electric field plot from top monitor for a normal p-i-n structure on substrate.

Figures 3.6 (a) and (b) depict the LEE vs radius and LEE vs spacing, with the dipole being placed at the center of the active region and a monitor above the LED structure. Shown in Figure 3.6 (a), LED2 demonstrated an enhancement in the LEE when compared to LED1 because of the shorter distance between the active region and the Si substrate, consequently stronger reflection from substrate. When compared to the light absorptive properties of silicon material, flip-chip LEDs with light reflective mirrors has been reported to have an enhanced LEE [40] [3] [22]. The aforementioned argument has been used to support the fact that LED3 has a higher

LEE attributed to the presence of a stronger reflection of light from Cu, and also due to the reduced absorption in Cu as compared to Si substrate [3]. The stronger reflection ensures a higher probability of the light generated by the active region to be reflected back from the substrate, which is eventually extracted after multiple total internal reflections inside the LED structure. The LEE of LED3 is enhanced when compared to LED2 due to the minimized absorption of propagating light to Cu when compared to Si [3]. Moreover, the presence of a metal layer also ensures the formation of a better ohmic contact at the p-type region [40].[3] Illustrated in Figure 3.6, flip-chip LED3 exhibits highest LEE compared to LED1 and LED2, in virtue of the shorter distance between the active quantum well region and the metal reflector. The p-type metallization employed in flip-chip LEDs served the purposes of an ohmic contact, optical reflector and a current spreading layer [3].

Variation of critical parameters such as radius and spacing between nanowires play an important role on LEE. As shown in Figure 3.6, there is an optimum radius and spacing to avoid photonic bandgap and have high LEE. The electric field plots depicted in Figures 3.6(c) and (d) shows the electric field distribution for both the flip-chip structures on Cu and typical structure mounted on Si substrate. Both flip-chip structures refer to regular periodic structures with a radius of 50 nm and center to center spacing of 130 nm. Figure 3.6(c) shows that in the flip-chip structure, the light is not locally stagnant, rather much better propagated within the structure. In other words as compared to a conventional LED device composed of multiple nanowires, there is a contribution from majority of nanowires within the device towards light extraction, as opposed to a normal p-side up structure on Si substrate where light extraction is typically concentrated towards the center and a minority of nanowires (placed in the middle of the device) contributes to the light extraction.

As seen in the SEM image depicted in Figure 3.8, the SEM image shows some randomness in the fabricated structure. We have considered this in the FDTD

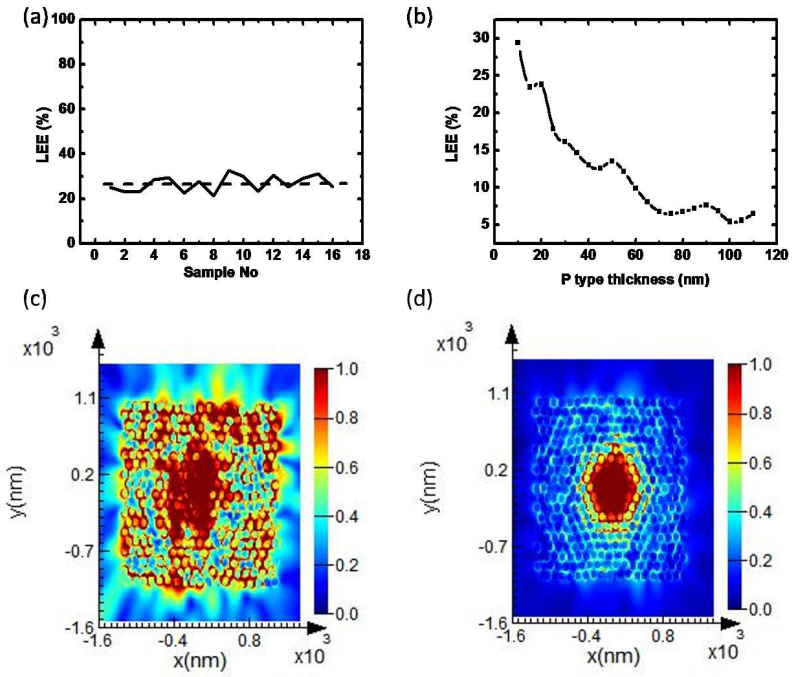

Figure 3.7 (a) LEE for 16 different random structures with different nanowire diameter and nanowire spacing between them. (b) Variation of p-type height with LEE of a flip chip (n-i-p) structure on metal (c) and (d) Electric field contour plots for a typical random flip chip structure on metal and a random normal (p-i-n) structure on substrate.

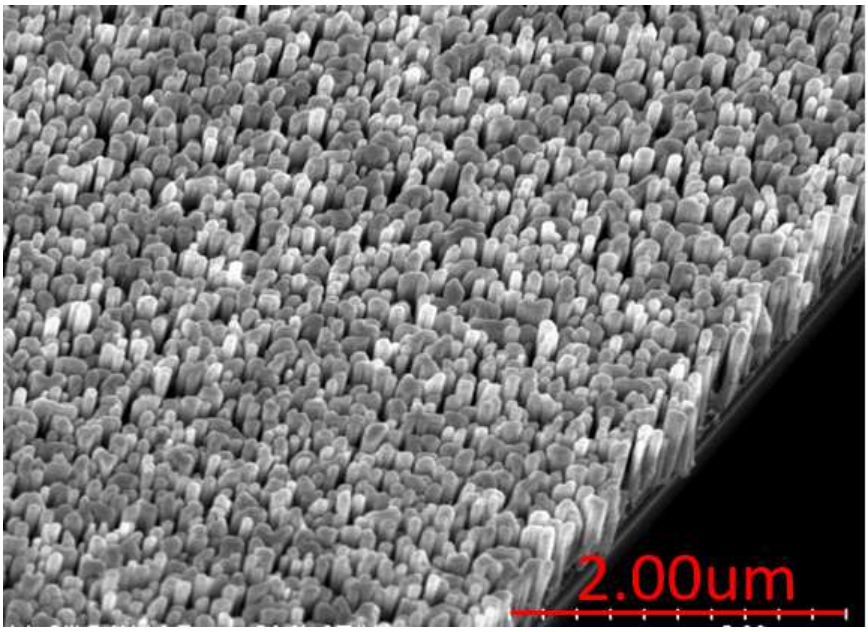

Figure 3.8 SEM image of nanowire LEDs on SOI substrate.

simulations. Radius of 50 nm and centre to centre spacing of 130 nm with a tolerance of ±5% was used to run our simulations.

Figure 3.7(a) represents the LEEs of 16 typical random flip-chip structures with different nanowire radius and spacing, similar to the ones we do fabricate. To account for the randomness from the periodic structure arrangement, which may arise due to various steps during the fabrication route, a thorough quantitative measure in terms of LEE between a periodic and a random structure was analyzed. In view to the above approach, the radius ranges from 47.5 nm to 52.5 nm (deviation from 50 nm radius) and center to center spacing ranges of 125 nm 135 nm (deviation from 130 nm spacing) were considered. The LEE of the flip structure at a radius of 50 nm and a spacing 130 nm was 9.61%, while the random structure has an average LEE of 26.79%. From the perspective of practical feasibility when fabricating nanowires and its dependence on LEE, a total of 10% fabrication tolerance was provided and the above was investigated for 16 different random structures. The datum point we have chosen for providing the 5% allowance is basically the radius of the nanowire (50 nm) and the center to center spacing between the nanowires (130 nm). Deviation in LEE for the random structure from the periodic structure was thus sought off, in regard to the flip chip arrangement.

In the case considered here, the random structure offers better LEE than a normal pin structure. For periodic structures the device will work in the photonic band gap (PBG) mode, while for the same amount of randomness in a random structure there is the probability of device working outside the scope of PBG modes. The latter enhanced LEE of 26.79% in random structures in contrast to the periodic structures LEE of 9.61% for a nanowire arrangement of 50 nm radius and spacing 130 nm can also be explained by the probability of majority distribution of nanowires towards the optimized radius. In other words, the large change in slope of LEE characteristics in flip chip structure and distribution of more nanowires closer to the

optimized radius might have contributed to the disparity of enhanced LEE in random structure over regular periodic structure. Even with the randomness in the structure, LEE thus shows a similar trend for both the flip chip and the normal structure supporting our claim.

Figure 3.7(b) depicts the effect the p-GaN thickness on LEE of a flip chip device structure. Modification in p-GaN thickness of nanowire has a sizable contribution to the LEE. Figure 3.7 thus shows the LEE into air at 550 nm with the dipole source being placed at the middle of the active region for varying p-GaN thicknesses. P-GaN shows a strong variation in trend of light extraction efficiency with p type thickness. LEE vs p type thickness shows a sinusoidal behaviour, almost similar to the transmittance curve we see in Fabry-Perot etalon. The latter behaviour is explained by the superimposition/interference effect between the forward and backward travelling photons [9]. The latter reaffirms the necessary constraints for constructive reflection occurring within the active region of the nanowire. This in turn stresses the need for optimizing the p-type layer thickness for the best LEE. Compared to previously mentioned parameters, the p-GaN shows a strong variation in light extraction efficiency. It is even worse for smaller thickness because of the high reflection from reflective layer on the top of substrate.

Figures 3.7 (c) and 3(d) represents the electric field contour plots of a random flip chip on metal and random normal p-i-n structure on substrate. As in the case depicted in Figures 3.6(c) and (d) periodic nanowire structures, the distribution of contribution towards light extraction remains the same in random flip-chip and random p-i-n structures, illustrated in Figures 3.7(c) and (d).

3.3.1 Measurements and Results

Shown in the first plot in Figure 3.9, after being transferred to Cu substrate, the PL intensity of nanowires is enhanced by a factor of 1.5 compared to that of as-grown

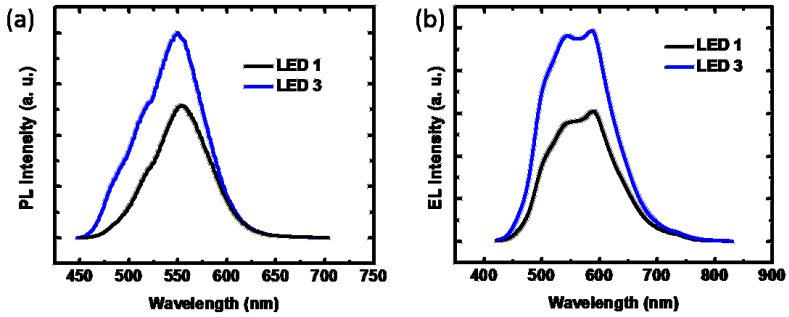

Figure 3.9 EL (a) and PL (b) measurements of flip chip on copper and normal structure on silicon substrates.

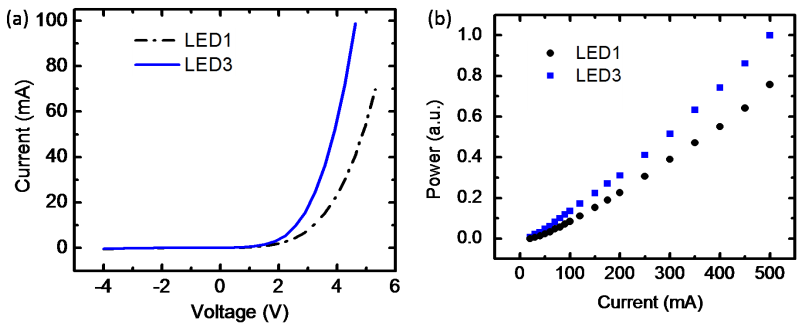

Figure 3.10 I-V (a) and P-I (b) characteristics of LED 1 and LED 3 devices.

nanowire LEDs on SOI substrate. Such enhancement is mainly attributed to the improved light extraction efficiencies due to the significantly reduced light absorption after removing the Si substrate. Moreover, the Ni/Au bi-layer may work as a reflector to further enhance the LEE. This further confirms that the nanowire damage during the transferring process is almost negligible. The electroluminescence intensity of the LED3 measured was of nearly twice higher than that of the regular nanowire LED on Si (LED1), shown in Figure 3.9 second figure. Such enhanced PL and EL intensities agree well with the simulation results presented in Figures 3.6 and 3.7.

Figure 3.10, first plot, shows the current-voltage characteristics of a nanowire LED on Cu compared to a similar nanowire device on Si substrates. The LEDs on Cu substrate exhibit excellent current-voltage characteristics and show slightly higher current, compared to the LED device on Si substrate at the same voltage. At 20mA injection current, the operation voltages for LED on Cu and LED on Si substrate are 2.9 V and 3.7 V, respectively. The lower operation voltage may be attributed to the better heat dissipation and substrate conductivity of the nanowire LED on Cu substrate which is consistent with other reports. Shown in the inset, the optical image of light emission from the LED device on Cu substrate, demonstrating the successful fabrication of such nanowire of on metal substrates. Figure 3.10. second plot, shows the relative light output power of both LED1 and LED3 for comparison. It is shown that LED3 exhibit stronger output power compared to that of LED1. Such output power enhancement is attributed to the enhanced LEE in LED3 which was explained previously. To further increase the output power of LED3, several limiting factors should be considered, for instance, improving the transparency of the top Ti/Au top metal contact and optimizing the nanowire geometry including wire density, diameter, and height.

We have further developed phosphor-free white LEDs on Cu substrate by manipulating the In composition in the InGaN active region, thereby, white light

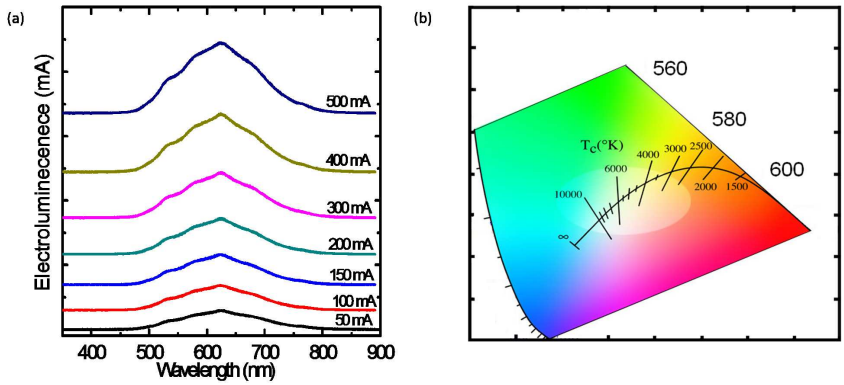

Figure 3.11 EL spectrum (a) and CIE diagram (b) of phosphor free white LEDs on Cu substrate.

emission with full visible spectrum is achieved. Figure 3.11, first plot, shows the EL spectra of phosphor-free white-LEDs on Cu substrate under different injection current. The peak wavelength is almost stable when current increases from 50mA to 500mA attributed to the low quantum confined Stark effect. Moreover, the LED device achieves stable white light emission on CIE diagram, shown in Figure 3.11, second plot. The device achieves high CRI of 95 showing promise as a candidate for solid-state lighting and display.

3.4 Conclusion

In summary, we have been able to grow full-color nanowire LEDs, with the incorporation of InGaN/AlGaN nanowire heterostructures, directly on the Si (111) substrates by MBE and successfully change the color of emitted light by changing the composition of indium on the quantum well of the LED NW.

In addition, we have transferred high performance nanowire LEDs on Cu substrates via substrate-transfer process and in doing so have proven that the output power and light extraction efficiency is higher when compared to NW LEDs grown on silicon.

CHAPTER 4

UV NANOWIRE LIGHT-EMITTING DIODES OPERATING IN THE UV-B RANGE

4.1 Introduction

The fabrication of a $GaN/Al_xGa_{1-x}N$ vertically aligned nanowire based double heterojunction LED on silicon substrate by MBE is reported. Peak emission wavelength in the UV-B range which is from 290 to 300 nm has been demonstrated for these highly efficient $GaN/Al_xGa_{1-x}N$ nanowire array based LEDs. The EL spectra further depicts the stable light emission nature (no red or blue shift) from the LED device. The experimental results are backed up by simulation, using FDTD solution.

Optoelectronic devices operating in the ultraviolet (UV) spectral region have presented themselves with enormous potential in the medical field. The UV-B light emitters are widely used for phototherapy. Phototherapy involves treatment of the skin, by exposing it to a UV-B source of light. This procedure is used to treat various diseases ranging from skin cancer, psoriasis, stimulating wound healing, stimulating the immune system and DNA analysis. This particular spectrum has also found its use almost exclusively in the skin tanning industry. The UV-B source of light, when incident to the skin, activates a pigment called melanin, which aids or accelerates the process of tanning.

Devices used traditionally for producing UV spectra of light are large and bulky, like UV lamps consisting of mercury. These devices exhibit low efficiency and lack of flexibility as well. These issues can be resolved using nanowire LEDs, which have flexible device size, ranging from a single nanowire to a nanowire array. Nanowire LEDs serve as waveguides which lead to high efficiency emissions that save the trouble of complicated packaging and the requirement of reflectors and lenses. ZnO or ZnO/GaN heterostructures are currently used to fabricate UV LEDs.

However, these devices exhibit high operating voltage, a very large and unusable resistance (1000 ohm or higher), and an uncontrolled emission wavelength, accounting to p-type ZnO being unstable, the lack of carrier confinement, and the interfacial defects between ZnO and GaN. These devices have not reported quantum efficiency either. The approach using highly efficient AlGaN nanowire heterojunction structures proves to be a useful alternative. AlGaN quantum wells have been used to produce light in the UV-B range of light. The issue of p-type doping can be addressed by employing novel designs such as, tunnel junction, polarization enhanced Mg doping of AlGaN/GaN superlattices, and polarization induced holes in an Al compositionally graded junction. The growth of near defect free high quality AlGaN nanowires with controlled directionality, uniformity, and tenability of the Al compositions prove to be a difficult task. Use of a metal catalyst could severely degrade the optical and electrical properties of the devices. There is also the issue of the absence of effective carrier localization effect, hence carriers can easily migrate to the surface of nanowires and this non radiative recombination on the sidewall of nanowires caused by surface states/defects severely limits the device efficiency.

4.1.1 Simulation Device Model

In view of the above, we have developed a unique nanowire LED heterostructures for the purpose of emitting light in the UV-B range. The design of the nanowire LED array is shown schematically in Figure 4.1. The array is in abab (hexagonal) structure. Each nanowire consists of 250 nm n-GaN, 100 nm n-AlGaN, 60 nm MQW, 100 nm p-AlGaN and 10 nm p-GaN. The underlying substrate is Si (110). We have used three dimensional FDTD simulation, to analyze and calculate the light extraction efficiency of the nanowire LEDs. The device spans $2.5\mu m \times 2.5\mu m$, enclosed in 12 perfectly matched layers (PML) to absorb outgoing waves without causing any reflection. The parameters of PML (σ) (attenuation factor) and (κ) (auxiliary attenuation coefficient)

are set to 0.25 and 2 respectively. Via adaptive meshing technique, the minimum mesh step size was set to 0.25. The source to replicate the excitation was a single dipole source with Gaussian shape spectrum, and TM mode (electric field parallel to nanowire axial direction) is placed in the nanowire in the middle of the nanowire array, in the middle of the active region. The simulation wavelength varies from 290 nm, 300 nm and 320 nm. The light extraction efficiency is calculated with the help of Poynting vectors in the path shown as solid yellow lines (the monitors) as shown in Figure 4.1. The ratio of the power emitted from the side surfaces of the LED to the total emitted power of the device active region is the LEE. Figure 4.2 is an illustration of a 3-D iso-view of the nanowire array. Such nanowires can be grown by MBE. Figure 4.2 shows a 3-D representation of the nanowire array in its abab formation. Figure 4.3 shows the 3-D schematic structure of each nanowire used in the array. Figure 4.4 shows the SEM image of a sample of fabricated device.

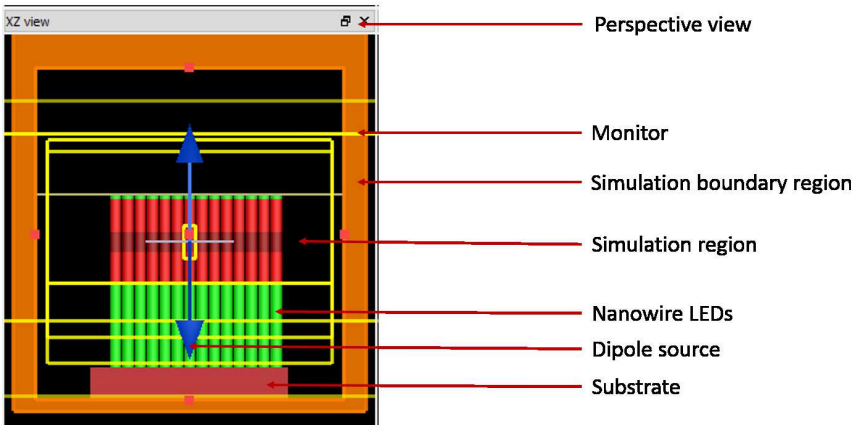

Figure 4.1 FDTD Lumerical design of UV-B nanowire array.

4.2 Simulation Results

To understand the dependency of LEE on the nanowire parameters like radius and spacing, 3 contour plots, as shown in Figures 4.5, 4.6 and 4.7, relating these three parameters can be seen in the aforementioned figures. Nanowire parameters critically affect the lateral light extraction efficiency. A relatively high LEE of 23.43% is

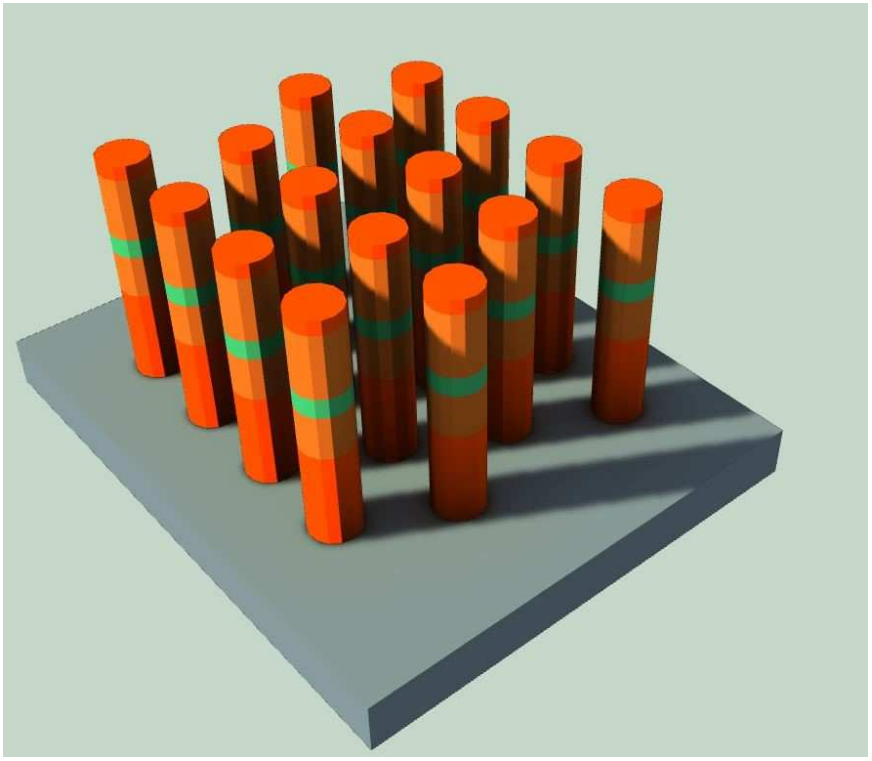

Figure 4.2 3-D schematic of UV-B nanowire LED array.

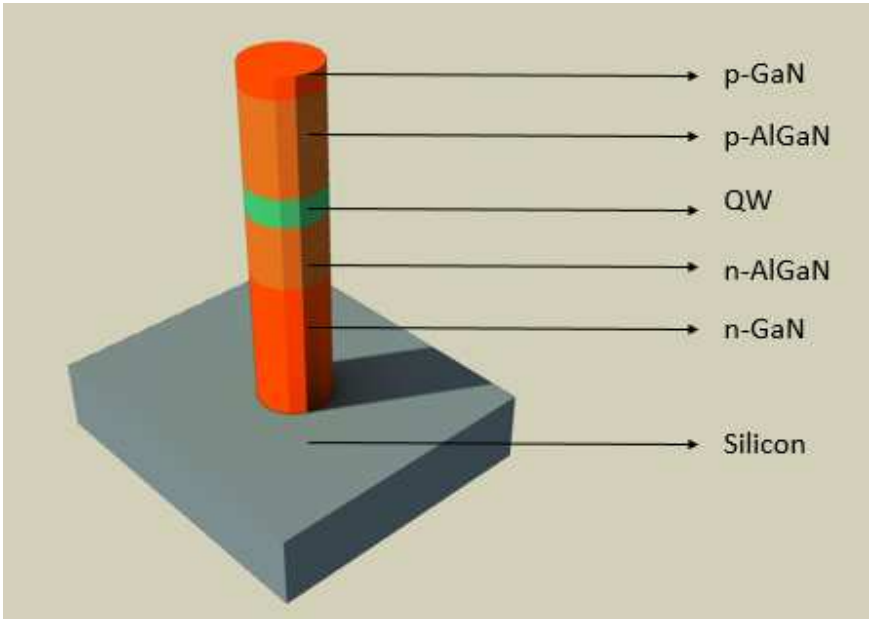

Figure 4.3 3-D schematic of UV-B nanowire LED.

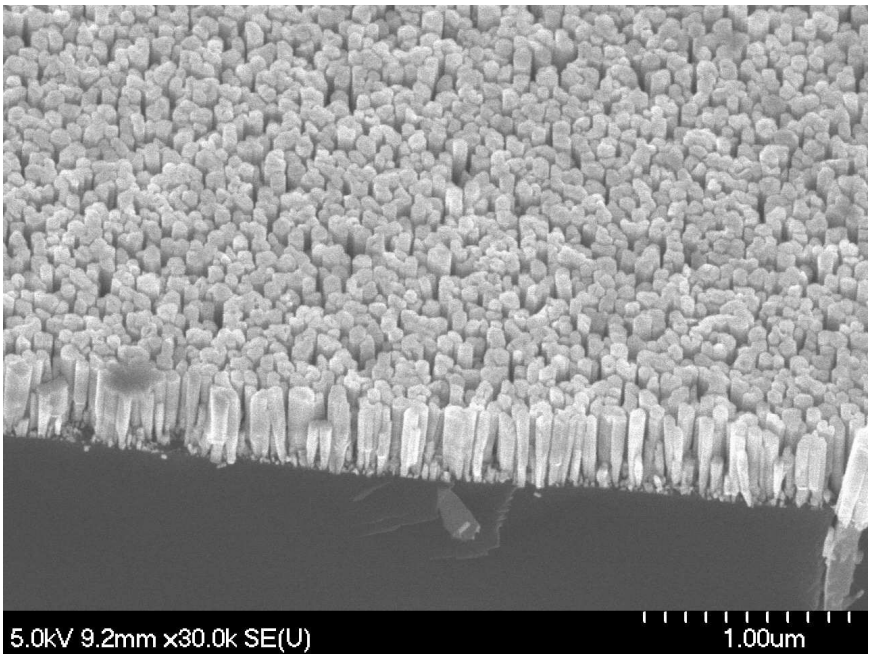

Figure 4.4 SEM image of UV-B nanowires on Si.

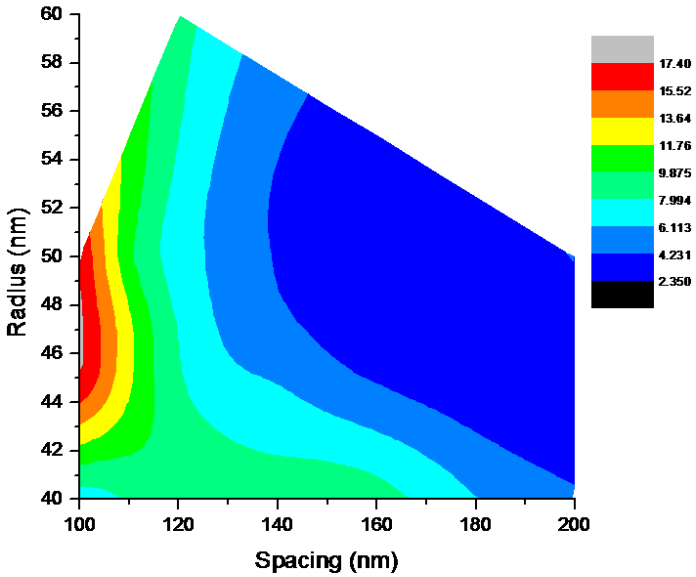

Figure 4.5 Contour map showing variation of light extraction efficiency with change in nanowire spacing and radius at 290 nm.

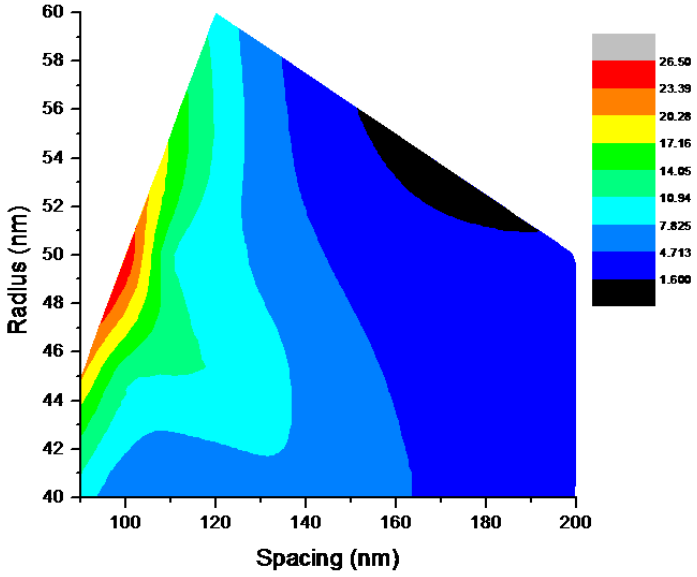

Figure 4.6 Contour map showing variation of light extraction efficiency with change in nanowire spacing and radius at 300 nm.

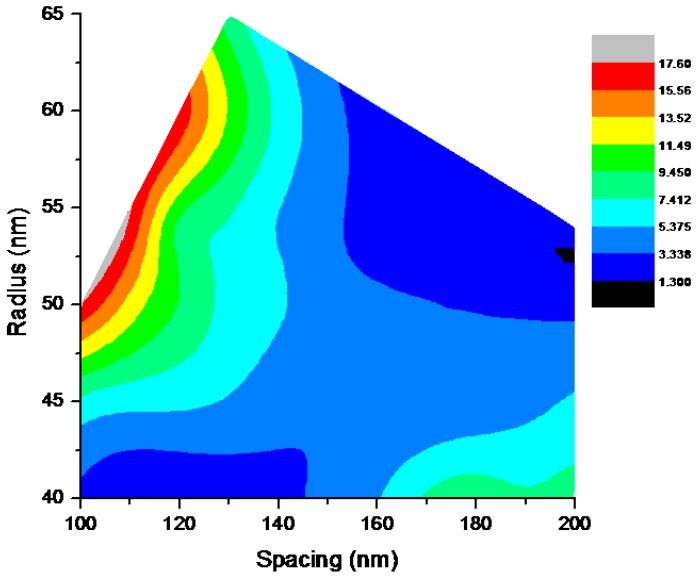

Figure 4.7 Contour map showing variation of light extraction efficiency with change in nanowire spacing and radius at 320 nm.

acquired at a spacing of $100nm$ and radius of $50nm$ for emission at wavelength equal to 300 nm as a peak among all our simulations. A peak of 17.37% at 100 nm spacing and 50 nm radius for emission at 290 nm and a peak of 17.58% at 100 nm spacing and 50 nm radius is found.

We have used the simulation results to fabricate devices of around this range of nanowire spacing and radius for maximum possible LEE extraction.

The nanowire LED array periodic structure is very similar to the active photonic crystal structures. However, photonic crystals themselves are utilized in photonic bandgap regions whereas the nanowire LED periodic array is utilized in the non-bandgap regions. Photonic bandgap regions are sets of wavelength prohibited from propogating throughout the structure. Since the nanowire LED array prefer non-bandgap regions, light propagates through the structure into surrounding air. [7]

Depending on the need of application, the nanowire photonic crystal structures have different operating regimes, namely, light confinement regime, which is used for LASERS, and light transmission regime, used in LEDs Depending on nanowire diameter and spacing. Nanowire with varying diameter and spacing result in the formation of different wave vectors, and hence different degrees of transmission at corresponding wavelengths.

The FDTD simulation utilized to acquire information about LEE of different nanowire array diameter and spacing uses particle swarm optimization (PSO). As seen in the plot, we have acquired a peak LEE of 20% for nanowire spacing and radius of 110 nm and 45 nm respectively. Here, the spacing is center to center spacing between two adjacent nanowires.

The lateral light extraction that is observed in the LED nanowire array can be accounted for by the coupling of light modes through the nanowire's in the photonic non-bandgap transmission region which supports the light propagation inside the structure.

Therefore, careful control over spacing and radius is to be exercised to endure least possible total internal reflection at the semiconductor-air interface, which would aid the light to escape the device leading to a higher LEE. [7]

The effect of change in spacing and radius can be seen by examining the contour plot. The LEE varies from 2.0% to 26%. The reason for this can be accounted to the formation of coupled modes, leading to a jump in LEE.

4.3 Experiments and Results

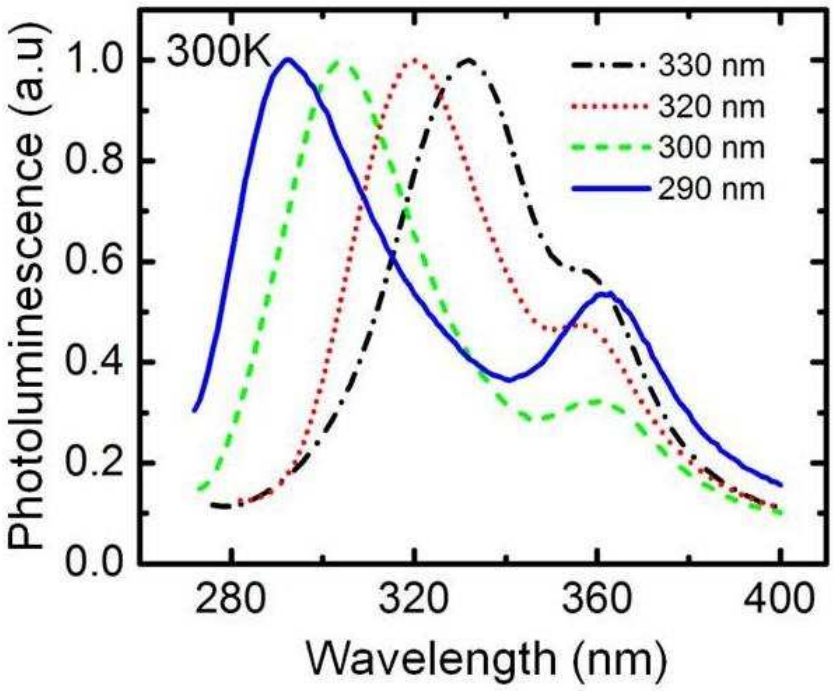

Figure 4.8 Photoluminescence versus wavelength of UV-B nanowires.

Optical properties of GaN/AlGaN nanowire LEDs were examined using a 266 nm diode-pumped solid-state (DPSS) Q-switched laser as the excitation source. To eliminate the emission from the excitation laser source, a long pass filter ($> 270nm$) was placed in front of the spectrometer. The graph shows 4 plot of nanowire LEDs fabricated emitting 290 nm, 300 nm, 310 nm, 320 nm respectively, measured at 300

K. As seen from the corresponding plots, the peaks match the designed wavelength of the light excited from the nanowire LEDs. The plot can be seen in Figure 4.8.

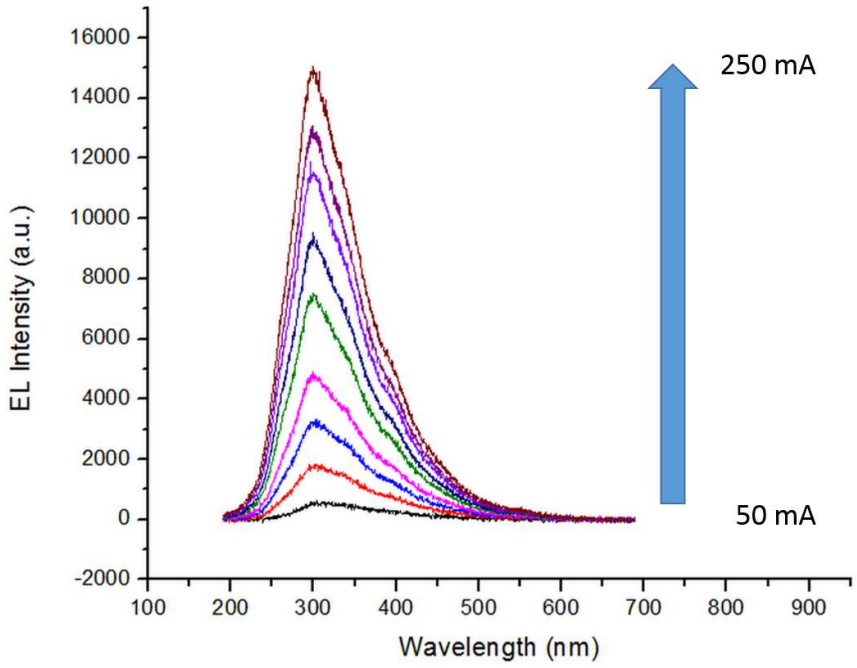

Figure 4.9 Electroluminescence versus wavelength of UV-B nanowires.

The EL spectra of the nanowire LEDs were measured at room temperature using the Ocean Optics spectrometer (USB 2000) at injection currents varied from 30 mA to 120 mA. The EL spectra exhibits a singular peak at around 310 nm which corresponds to the emission from the multiple AlGaN quantum wells. It can be seen that the device shows a stable and strong emission at 310 nm with the absence of emission on the visible wavelength range which was observed in AlGaN MQW based UV LEDs, due to the deep level defects in AlGaN .This clean EL spectrum is crucial in the improvement of the signal-noise ratio. Additionally, the emission peak position shows very small shifts with increasing injection current, emphasizing the presence of a negligible polarization field due to the effective strain relaxation in the lateral direction of nanowires. The plot can be observed in Figure 4.9.

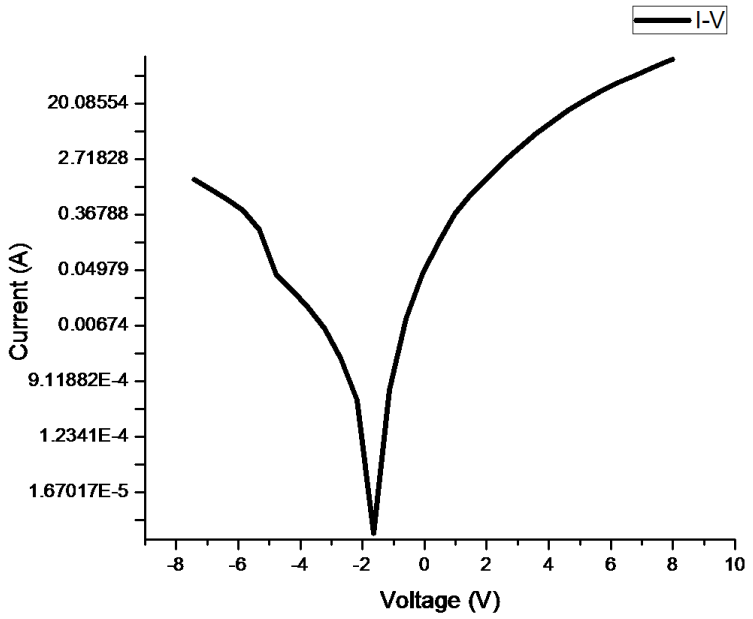

Figure 4.10 Current versus voltage of an AlGaN/GaN LED emitting light in UV-B range.

Figure 4.10 shows a typical I-V curve, for nanowire based UV LEDs with an area of $300\mu m \times 300\mu m$. The device shows excellent diode characteristics under forward bias, with 6.2 V at 42 mA injection current. The series resistance is estimated to 26Ω. The leakage current under a reverse bias of around -7 V is around 1 A. Such results are significantly better than other thin film based LEDs in the UV region. Achieving such good electrical properties for the nanowire LED devices can be partly accounted to the enhanced conductivity in III-nitride nanowires, due to the significant reduction in the formation energy for substantial doping in the near surface region of nanowires.

4.4 Conclusion

In summary, we have demonstrated a method which can improve the efficiency of existing UV-B devices using novel AlGaN nanowire LEDs on a silicon substrate. The LEE has been significantly improved in this device due to the designed arrangement

pf nanowire geometry. These devices can be used for medical applications which utilize the UV-B range of spectra.

CHAPTER 5

POTENTIAL APPLICATIONS

5.1 Deep UV LEDs Operating in 210-280 nm: Device Applications and Device Structure

Group III-nitride UV LEDs have gained considerable interest due to a number of applications, e.g., water purification, disinfection of medical tools, UV curing, document authentication, phototherapy and medical diagnostics [13]. Each of these applications requires light sources emitting at a different UV wavelength. For example, in the case of water purification systems, the water is irradiated with UV light to clear microorganisms such as bacteria, viruses and spores. The radiation disrupts chemical bonds within the DNA or RNA of the microorganism so that they are unable to replicate and, thereby, are rendered inactive. The optimum wavelength can vary slightly depending on the microorganism, but particularly light in the wavelength range from 200 to 300 nm is most suitable with a pronounced maximum at about 265 nm. The first UV LED-based water purification system, applicable for either standing or running water, was recently demonstrated [33] [37].

We have been working on designing a structure that would be useful in developing nanowire LEDs that emit light in the deep UV range of spectra. Figure 5.1 illustrates a schematic of the structure of this nanowire LED which emits light at 240 nm.

Table 5.1 shows the refractive indices of the materials used.

We have conducted preliminary FDTD simulations for the structure shown in Figure 5.1. This device would help us in designing UV filters for water purification purposes. The challenge in implementing these devices are in treating large volumes of water, as small amounts can be treated at a time now, and UV LED sources still suffer from relatively low external quantum efficiencies and emission power.

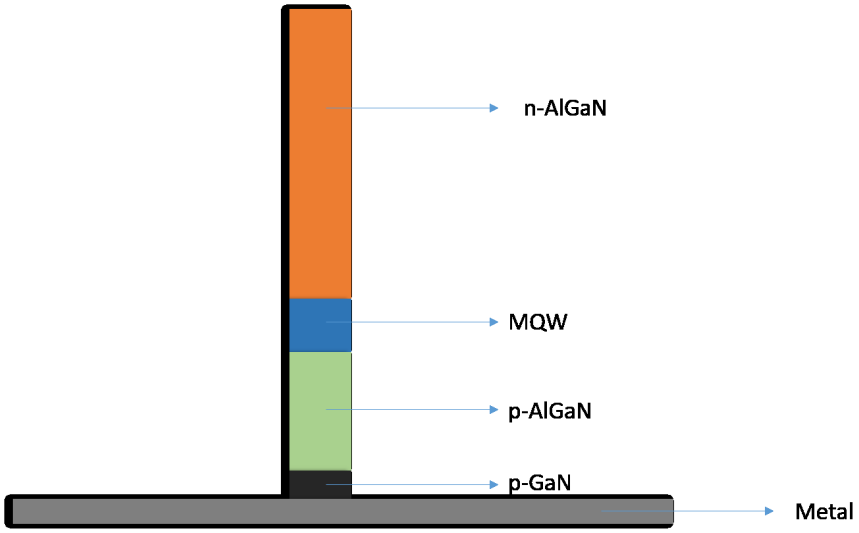

Figure 5.1 Schematic diagram of UV LED operating at 240 nm.

Table 5.1 Refractive Indices and Height of Materials used

	Material	*Refractive Index*	*Height (nm)*
(i)	n-AlGaN	2.45	400
(ii)	MQW	2.55	60
(iii)	p-AlGaN	2.45	100
(iv)	p-GaN	2.7	10

5.2 Deep Ultraviolet Laser diodes

Currently, the main focus of III-nitride research is the realization of an electrically injected laser diode which can operate at the deep UV wavelength range. Researchers have been working on the optimization of design for vertical cavity surface-emitting lasers and edge emitting lasers on various substrates. Deep UV nanowire laser diodes is a very new challenge. There haven't been many reported nanowire laser diodes that operate at this wavelength.

We have come up with a structure, as can be seen in Figure 5.2, that may provide a solution to this wavelength. Using the same nanowire structure for deep UV LEDs, and keeping the nanowire array in between DBR (distributed bragg reflector) structures. We have run simulations using this design in mind to try to impart lasing action in our nanowire structure. Figure 5.2 shows the schematic for this design. [29]

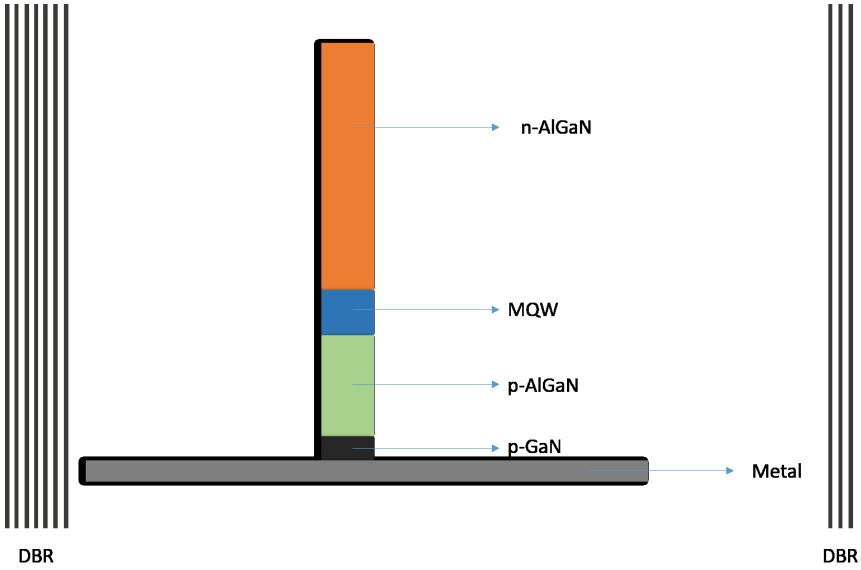

Figure 5.2 Schematic illustration of UV laser diode operating at deep UV range.

We have implemented theoretical studies and preliminary simulation using aforementioned structure. The main issue with laser diodes at this wavelength achieving stimulated emission, which can be done using optical pumping and not by current injection.

5.3 Visible Light-emitting Diodes for Wearable Electronics

Flexible and stretchable conductive fibers have received significant attention due to their properties, which can be used for wearable and fold-able electronics.

Wearable electronics is a field of engineering that has raised much attention in the photonics industry. The recent big players in the industry have heavily invested in this technology, and thus has made tremendous progress. Examples include flexible and stretchable circuitries, flexible displays, flexible energy devices, smart skins, electronic eye type imagers, soft and human friendly devices, and so on. [15]

The stretchable and flexible electronics have been developed by two main strategies:

- engineering new structural constructs to form conventional established materials
- assemble a device from stretchable newly developed nanomaterials

We have reported nanowire LEDs on multiple types of substrates like metals and silicon. There is also research being done on growing nanowire LEDs on flexible substrates like polymers. This would enable incorporating high performance nanowire LED devices in wearable electronics. Large manufacturers like Samsung and Apple have been tackling this industry and nanowire LEDs could provide a reasonable solution.

This field is a cutting-edge technology and a novel idea. Much work and effort has to be put into the eventual large scale production at an industry level for these devices, which will transform the way LEDs can be used in our day to day lives.

BIBLIOGRAPHY

[1] *Understanding the Finite-Difference Time-Domain Method.* www.eecs.wsu.edu/ schneidj/ufdtd, 2010.

[2] Shamsul Arafin, Xianhe Liu, and Zetian Mi. Review of recent progress of iii-nitride nanowire lasers. *Journal of Nanophotonics*, 7(1):074599–074599, 2013. 10.1117/1.JNP.7.074599.

[3] A. L. Bavencove, G. Tourbot, J. Garcia, Y. Dsires, P. Gilet, F. Levy, B. Andr, B. Gayral, B. Daudin, and Dang Le Si. Submicrometre resolved optical characterization of green nanowire-based light emitting diodes. *Nanotechnology*, 22(34):345705, 2011.

[4] M. Bertelli, P. Lptien, M. Wenderoth, A. Rizzi, R. G. Ulbrich, M. C. Righi, A. Ferretti, L. Martin-Samos, C. M. Bertoni, and A. Catellani. Atomic and electronic structure of the nonpolar $GaN(1\bar{1}00)$ surface. *Physical Review B*, 80(11):115324, 2009. PRB.

[5] S. Chevtchenko, X. Ni, Q. Fan, A. A. Baski, and H. Morko. Surface band bending of a-plane gan studied by scanning kelvin probe microscopy. *Applied Physics Letters*, 88(12):122104, 2006.

[6] Faqrul A. Chowdhury, Zetian Mi, Md G. Kibria, and Michel L. Trudeau. Group iii-nitride nanowire structures for photocatalytic hydrogen evolution under visible light irradiation. *APL Materials*, 3(10):104408, 2015.

[7] Mehrdad Djavid and Zetian Mi. Enhancing the light extraction efficiency of algan deep ultraviolet light emitting diodes by using nanowire structures. *Applied Physics Letters*, 108(5):051102, 2016.

[8] Yajie Dong, Bozhi Tian, Thomas J. Kempa, and Charles M. Lieber. Coaxial group iiinitride nanowire photovoltaics. *Nano Letters*, 9(5):2183–2187, 2009.

[9] Martin A. Green and Mark J. Keevers. Optical properties of intrinsic silicon at 300 k. *Progress in Photovoltaics: Research and Applications*, 3(3):189–192, 1995.

[10] Wei Guo, Meng Zhang, Pallab Bhattacharya, and Junseok Heo. Auger recombination in iii-nitride nanowires and its effect on nanowire light-emitting diode characteristics. *Nano Letters*, 11(4):1434–1438, 2011.

[11] Justin C. Johnson, Heon-Jin Choi, Kelly P. Knutsen, Richard D. Schaller, Peidong Yang, and Richard J. Saykally. Single gallium nitride nanowire lasers. *Nat Mater*, 1(2):106–110, 2002. 10.1038/nmat728.

[12] Deepak L. N. Kallepalli, Ali M. Alshehri, Daniela T. Marquez, Lukasz Andrzejewski, Juan C. Scaiano, and Ravi Bhardwaj. Ultra-high density optical data storage in common transparent plastics. *Scientific Reports*, 6:26163, 2016.

[13] M. Kneissl, T. Kolbe, C. Chua, V. Kueller, N. Lobo, J. Stellmach, A. Knauer, H. Rodriguez, S. Einfeldt, Z. Yang, N. M. Johnson, and M. Weyers. Advances in group iii-nitride-based deep uv light-emitting diode technology. *Semiconductor Science and Technology*, 26(1):014036, 2011.

[14] A. Laubsch, M. Sabathil, J. Baur, M. Peter, and B. Hahn. High-power and high-efficiency ingan-based light emitters. *IEEE Transactions on Electron Devices*, 57(1):79–87, 2010.

[15] Phillip Lee, Jinhwan Lee, Hyungman Lee, Junyeob Yeo, Sukjoon Hong, Koo Hyun Nam, Dongjin Lee, Seung Seob Lee, and Seung Hwan Ko. Highly stretchable and highly conductive metal electrode by very long metal nanowire percolation network. *Advanced Materials*, 24(25):3326–3332, 2012.

[16] M. A. Mastro, B. Simpkins, G. T. Wang, J. Hite, Jr. Eddy, C. R., H. Y. Kim, J. Ahn, and J. Kim. Polarization fields in iii-nitride nanowire devices. *Nanotechnology*, 21(14):145205, 2010. 1361-6528 Mastro, Michael A Simpkins, Blake Wang, George T Hite, Jennifer Eddy, Charles R Jr Kim, Hong-Youl Ahn, Jaehui Kim, Jihyun Journal Article Research Support, U.S. Gov't, Non-P.H.S. England Nanotechnology. 2010 Apr 9;21(14):145205. doi: 10.1088/0957-4484/21/14/145205. Epub 2010 Mar 11.

[17] Andrew McCague, Adam Schulte, and Joseph Vivian Davis. Scapulothoracic dissociation: An emerging high-energy trauma in medical literature. *Journal of Emergencies, Trauma, and Shock*, 5(4):363–366, 2012. JETS-5-363[PII] 23248512[pmid] J Emerg Trauma Shock.

[18] Matteo Meneghini, Nicola Trivellin, Gaudenzio Meneghesso, Enrico Zanoni, Ulrich Zehnder, and Berthold Hahn. A combined electro-optical method for the determination of the recombination parameters in ingan-based light-emitting diodes. *Journal of Applied Physics*, 106(11):114508, 2009.

[19] H. P. Nguyen, M. Djavid, K. Cui, and Z. Mi. Temperature-dependent nonradiative recombination processes in gan-based nanowire white-light-emitting diodes on silicon. *Nanotechnology*, 23(19):194012, 2012. 1361-6528 Nguyen, Hieu Pham Trung Djavid, Mehrdad Cui, Kai Mi, Zetian Journal Article Research Support, Non-U.S. Gov't England Nanotechnology. 2012 May 17;23(19):194012. doi: 10.1088/0957-4484/23/19/194012. Epub 2012 Apr 27.

[20] H. P. T. Nguyen, S. Zhang, K. Cui, X. Han, S. Fathololoumi, M. Couillard, G. A. Botton, and Z. Mi. p-type modulation doped ingan/gan dot-in-a-wire white-light-emitting diodes monolithically grown on si(111). *Nano Letters*, 11(5):1919–1924, 2011.

[21] Hieu Pham Trung Nguyen. *Molecular Beam Epitaxial Growth, Characterization and Device Applications of III-Nitride Nanowire Heterostructures*. PhD thesis, McGill University, 2012.

[22] Hieu Pham Trung Nguyen, Kai Cui, Shaofei Zhang, Mehrdad Djavid, Andreas Korinek, Gianluigi A. Botton, and Zetian Mi. Controlling electron overflow in phosphor-free ingan/gan nanowire white light-emitting diodes. *Nano Letters*, 12(3):1317–1323, 2012.

[23] Joachim Piprek. *Chapter 1 - Introduction to Semiconductors*, pages 3–11. Academic Press, Boston, 2003.

[24] Joachim Piprek. Efficiency droop in nitride-based light-emitting diodes. *physica status solidi (a)*, 207(10):2217–2225, 2010.

[25] Dvid Andor Rcz. Why invest in energy efficiency? the example of lighting. *Journal of Environmental Sustainability*, 2012.

[26] B. A. Russell, N. Kellett, and L. R. Reilly. A study to determine the efficacy of combination led light therapy (633 nm and 830 nm) in facial skin rejuvenation. *J Cosmet Laser Ther*, 7(3-4):196–200, 2005. Russell, B A Kellett, N Reilly, L R Clinical Trial Journal Article England J Cosmet Laser Ther. 2005 Dec;7(3-4):196-200.

[27] Daniel S. Seidman, Jonathan Moise, Zivanit Ergaz, Arie Laor, Hendrik J. Vreman, David K. Stevenson, and Rena Gale. A prospective randomized controlled study of phototherapy using blue and blue-green light-emitting devices, and conventional halogen-quartz phototherapy. *J Perinatol*, 23(2):123–127, 0000.

[28] Hiroto Sekiguchi, Katsumi Kishino, and Akihiko Kikuchi. Emission color control from blue to red with nanocolumn diameter of ingan/gan nanocolumn arrays grown on same substrate. *Applied Physics Letters*, 96(23):231104, 2010.

[29] Nakamura Shuji, Senoh Masayuki, Nagahama Shin-ichi, Iwasa Naruhito, Yamada Takao, Matsushita Toshio, Kiyoku Hiroyuki, and Sugimoto Yasunobu. Ingan-based multi-quantum-well-structure laser diodes. *Japanese Journal of Applied Physics*, 35(1B):L74, 1996.

[30] N. Tansu, H. Zhao, G. Liu, X. H. Li, J. Zhang, H. Tong, and Y. K. Ee. Iii-nitride photonics. *IEEE Photonics Journal*, 2(2):241–248, 2010.

[31] Timo Donsberg Tomi Pulli. Advantages of white led lamps and new detector technology in photometry. *Light Sci Appl*, 2015.

[32] M. A. Tsai, P. Yu, C. L. Chao, C. H. Chiu, H. C. Kuo, S. H. Lin, J. J. Huang, T. C. Lu, and S. C. Wang. Efficiency enhancement and beam shaping of gan;ingan vertical-injection light-emitting diodes via high-aspect-ratio nanorod arrays. *IEEE Photonics Technology Letters*, 21(4):257–259, 2009.

[33] S. Vilhunen, H. Sarkka, and M. Sillanpaa. Ultraviolet light-emitting diodes in water disinfection. *Environ Sci Pollut Res Int*, 16(4):439–42, 2009. Vilhunen, Sari Sarkka, Heikki Sillanpaa, Mika Journal Article Research Support, Non-U.S. Gov't Germany Environ Sci Pollut Res Int. 2009 Jun;16(4):439-42. doi: 10.1007/s11356-009-0103-y. Epub 2009 Feb 11.

[34] Chris G. Van de Walle and David Segev. Microscopic origins of surface states on nitride surfaces. *Journal of Applied Physics*, 101(8):081704, 2007.

[35] G. T. Wang. Iii-nitride nanowires for uv-visible optoelectronics. In *2015 IEEE Summer Topicals Meeting Series (SUM)*, pages 129–130.

[36] J. J. Wierer, G. T. Wang, Q. Li, D. D. Koleske, and S. R. Lee. Iii-nitride nanowire array solar cells. In *2012 Conference on Lasers and Electro-Optics (CLEO)*, pages 1–2.

[37] M. A. Wurtele, T. Kolbe, M. Lipsz, A. Kulberg, M. Weyers, M. Kneissl, and M. Jekel. Application of gan-based ultraviolet-c light emitting diodes–uv leds–for water disinfection. *Water Res*, 45(3):1481–9, 2011. 1879-2448 Wurtele, M A Kolbe, T Lipsz, M Kulberg, A Weyers, M Kneissl, M Jekel, M Journal Article Research Support, Non-U.S. Gov't England Water Res. 2011 Jan;45(3):1481-9. doi: 10.1016/j.watres.2010.11.015. Epub 2010 Nov 16.

[38] H Yamagishi, I Fusegawa, N Fujimaki, and M Katayama. Recognition of d defects in silicon single crystals by preferential etching and effect on gate oxide integrity. *Semiconductor Science and Technology*, 7(1A):A135, 1992.

[39] M. Zhang, P. Bhattacharya, J. Singh, and J. Hinckley. Direct measurement of auger recombination in in0.1ga0.9n and gan quantum wells and its impact on the efficiency of in0.1ga0.9n and gan multiple quantum well light emitting diodes. *Applied Physics Letters*, 95(20):201108, 2009.

[40] C. Zhao, T. K. Ng, A. Prabaswara, M. Conroy, S. Jahangir, T. Frost, J. O'Connell, J. D. Holmes, P. J. Parbrook, P. Bhattacharya, and B. S. Ooi. An enhanced surface passivation effect in ingan/gan disk-in-nanowire light emitting diodes for mitigating shockley read hall recombination. *Nanoscale*, 7(40):16658–65, 2015. 2040-3372.